



Li, L.-L., Lou, J.-L., Tseng, M.-L., Lim, M. K. and Tan, R. R. (2022) A hybrid dynamic economic environmental dispatch model for balancing operating costs and pollutant emissions in renewable energy: A novel improved mayfly algorithm. *Expert Systems with Applications*, 203, 117411. (doi: [10.1016/j.eswa.2022.117411](https://doi.org/10.1016/j.eswa.2022.117411))

There may be differences between this version and the published version. You are advised to consult the published version if you wish to cite from it.

<http://eprints.gla.ac.uk/269675/>

Deposited on 26 April 2022

Enlighten – Research publications by members of the University of Glasgow  
<http://eprints.gla.ac.uk>

## **A hybrid dynamic economic environmental dispatch model for balancing operating costs and pollutant emissions in renewable energy: A novel improved mayfly algorithm**

Authorship

### **Ling-Ling Li**

- State Key Laboratory of Reliability and Intelligence of Electrical Equipment, Hebei University of Technology, Tianjin 300130, China
- Key Laboratory of Electromagnetic Field and Electrical Apparatus Reliability of Hebei Province, Hebei University of Technology, Tianjin 300130, China

E-mail: [lilinglinghebut@126.com](mailto:lilinglinghebut@126.com)

### **Jia-Le Lou**

- State Key Laboratory of Reliability and Intelligence of Electrical Equipment, Hebei University of Technology, Tianjin 300130, China
- Key Laboratory of Electromagnetic Field and Electrical Apparatus Reliability of Hebei Province, Hebei University of Technology, Tianjin 300130, China

E-mail: [jjialehebut@126.com](mailto:jjialehebut@126.com)

### **Ming-Lang Tseng \***

- Institute of Innovation and Circular Economy, Asia University, Taiwan
- Department of Medical Research, China Medical University Hospital, China Medical University, Taichung, Taiwan

\* Corresponding author, E-mail: [tsengminglang@gmail.com](mailto:tsengminglang@gmail.com); [tsengminglang@asia.edu.tw](mailto:tsengminglang@asia.edu.tw)

### **Ming K. Lim**

- Adam Smith Business School, University of Glasgow, United Kingdom

Email: [Ming.Lim@glasgow.ac.uk](mailto:Ming.Lim@glasgow.ac.uk)

### **Raymond R. Tan**

- Department of Chemical Engineering, De La Salle University, Manila, Philippines

E-mail: [raymond.tan@dlsu.edu.ph](mailto:raymond.tan@dlsu.edu.ph)

## **A hybrid dynamic economic environmental dispatch model for balancing operating costs and pollutant emissions in renewable energy: A novel improved mayfly algorithm**

### **Abstract**

This study proposes a hybrid dynamic economic environmental dispatch model combining with thermal power units, wind turbines, photovoltaic and energy storage device to achieve the balance between operating cost and pollutant emission under the premise of stabilizing the output of renewable energy. Most studies have addressed economic and environmental issues to optimize dispatch as more and more renewable energy is connected to the grid, while ignoring the stability of renewable energy output. To solve the problem of instability of renewable energy output, a wind-photovoltaic stable output strategy is proposed and energy storage device is used to reasonably control the dispatch power of renewable energy. The fitness function is improved and an improved mayfly (IMA) algorithm using chaotic initialization, inertia weight and mutation strategy is proposed to find the optimal solution, and the performance of the algorithm is verified on two systems with different configurations. In addition, constraints such as the power balance, output of each generating device and energy of the energy storage device are considered. The results show that the operating cost of the IMA algorithm is 4.12%, 13.21% and 15.14% lower than those of the MA, MFO and PSO algorithms, and the proposed model using the IMA algorithm can effectively realize the balance of economic and environmental and obtain a stable output of renewable energy. This study provides a useful reference for the stable operation of power grid under a variety of renewable energy access conditions.

**Keywords:** Economic-environment dispatch; Wind-solar stable output strategy; Improved mayfly algorithm; Multi-renewable energy; Energy storage

# **A hybrid dynamic economic environmental dispatch model for balancing operating costs and pollutant emissions in renewable energy: A novel improved mayfly algorithm**

## **1. Introduction**

More countries to reduce the share of fossil fuels in their energy systems and to focus on the development and utilization of renewable energy such as wind, photovoltaic and tidal energy to address energy shortages and the greenhouse effect (Chen et al., 2020; Sun et al., 2021). The problems remain daunting despite the efforts of countries to achieve these goals through energy conservation and emission reduction. With significant impacts on industry and residential electricity consumption in many countries, the global outbreak of the COVID-19 epidemic has exacerbated the global energy crisis, reduced production from oil, coal and gas in exporting countries and led to a surge in prices (Heffron et al., 2021; Tseng et al., 2021). These crises demonstrate the necessity of the transformation from fossil fuel-based structure to renewable energy-based energy structure (Li et al., 2021a&b; Sun et al., 2021). At present, the global power generation is still dominated by thermal power, and nuclear power cannot be widespread due to its own limitations. It is necessary to increase the installed capacity and utilization rate of major renewable energy sources from wind power and photovoltaic, and further develop less pollutant emission technologies to ensure adequate and reliable electricity supply to reach the goal of net zero global energy carbon dioxide emissions and limit temperature rise to 1.5 °C by 2050 (IEA, 2021; WMO, 2020). In sum, the dynamic economic environmental dispatch (DEED) for energy and renewable energy is a common multi-objectives problem in power system dispatch (Evangeline and Rathika, 2021; Sundaram, 2020; Wang et al., 2021).

In recent years, wind turbines and photovoltaic devices have been connected to power system on a large scale. However, the increase of wind and photovoltaic generation power leads to the increases in dispatch cost of grid due to the uncertainty and uneven spatial and temporal distribution of these intermittent renewable energy generation (Hlalele et al., 2020). To assurance the stable operation of the power system, more thermal power units are added to the grid as spinning reserve for peaking. Energy storage device can effectively inhibit intermittent problem of wind and solar, adjust the output of the units with the development of energy storage technology, and can play a better role in peak shaving of power grid (Murphy et al., 2021; Nemati et al., 2018; Wu et al., 2019). Despite these advantages, electrochemical energy storage devices are not available in large quantities for grid dispatch at present due to high cost (Mazzoni et al., 2019; Tseng et al., 2021). The problem of grid dispatch is becoming more complex as renewable energy installations are increasingly added to grid, and therefore the use of energy storage facilities with certain capacity constraints to reasonably optimize the hybrid dynamic economic environmental dispatch (HDEED) containing renewable energy devices is a key issue for power system operators to be addressed. This study introduces a novel method to optimize operating cost and pollutant emission of electricity system considering wind, photovoltaic and energy storage devices to ensure the stability of renewable energy output while solving economic and environmental problems, and is for the stability of power system dispatch.

In view of these problems, this study combines wind, photovoltaic and thermal power units to optimize the HDEED problem and proposes an output strategy to address the instability of renewable energy generation, and combines with energy storage devices to improve the utilization rate of wind and photovoltaic power and ensure the stability output during dispatch cycle. In addition, this study proposes an improved mayfly algorithm (IMA)

into the dispatched model for high-dimensional, complex and multiple constraints. The two test systems are applied to validate the effectiveness of the modified optimization method. The contributions are as follows. (1) An integrated economic environmental dispatch model is proposed to deal with the optimization of units under more constraints in facing the multiple renewable energy outputs; (2) A Wind-photovoltaic stability output strategy is proposed to combine with energy storage devices, to improve the utilization rate of wind-photovoltaic, and ensure the stability of wind-photovoltaic power output in a dispatched cycle; (3) The fitness function is improved, and the improved function is compared to verify the better optimization effect; (4) An MA optimization algorithm is introduced into the model and improved according to the characteristics of the algorithm, which can effectively improve the convergence ability of the algorithm; and (5) The system combines with MA algorithm and control strategy has better effect in operating cost, emission and stability, which can effectively make up for the problem that practical stability is not considered when solving HDEED problems.

The rest of this study is organized as follows. Section 2 is the literature review and section 3 introduces the overall framework of the system to solve the HDEED problem, including the economic environmental dispatch model, the MA algorithm and its improved algorithm, and draws a clear system flowchart. Section 4 uses test function and comparison algorithms to verify the performance of the improved MA algorithm. Section 5 analyzes the effect of the proposed model by using two test systems. Finally, Section 6 summarizes the content of this study and future research prospects.

## **2. Literature review**

The economic environmental dispatch (EED) problem to be solved as the optimization of operating costs and pollutant emissions. For instance, Saenz et al. (2013) built a two-level decision-making framework to solve the EED problem, and developed a wavelet transform model for load demand forecasting and a particle filter model for generator dispatched. At same time, the active and reactive power balance of system are verified during optimized the operating costs and emissions; but lacks a penalty mechanisms in the load forecasting stage. Chen et al. (2019) analyzed the difference between pollutant emission and carbon dioxide emission and used a multi-objective scheduling model to control operating costs, CO<sub>2</sub> emissions and the distribution of multiple pollutants by analyzing the spatial and temporal distribution of pollutants, but better results may be achieved if combined with renewable energy. Sundaram (2020) studied the EED problem of a thermal power system containing heat and power unit and proposed an improved Multi-Verse algorithm to deal with constraint between the heat and power of the unit, and obtained the results from 140-bus system. Dong and Wang (2020) solved the static EED problem by using the feature that the robust algorithm does not need to adjust the hyper-parameters and transformed the nonlinear function into a high-dimensional linear function through the kernel trick for solving. The hyperparameter feature is needed to be adjusted for solving similar problems.

These studies that integrated operating cost and pollutant emission do not take renewable energy into account (Sun et al., 2021; Tseng et al., 2021). With the gradual transformation of energy structure and the maturity of renewable energy technology, the installed capacity of renewable energy in the power network is increasing, and many studies are taking renewable energy into account to solve the power grid dispatch problem. Studies involved renewable energy sources such as wind power and photovoltaics requires additional consideration of the volatility of power output. Most studies use Weibull function that

describes the probabilistic characteristics of wind speed to analyze the uncertainty of wind power ( de Siqueira and Peng 2021; Jin et al., 2018). The combination of day-ahead and real-time dispatch, the use of energy storage device to adjust the peak-valley difference, and the use of forecast error to analyze the risk level, are commonly used in renewable energy dispatch problem (Evangeline and Rathika, 2021; Li et al., 2020; Tan et al., 2020; Wu et al., 2019). These studies on the EED problem with renewable energy almost all analyze the uncertainty of wind and solar output to improve reliability.

DEED is a fundamental problem that needs to be solved in traditional power system. The aim is to find the corresponding power of each unit under minimum system cost, and many studies have already achieved better results for DEED problems(Jian et al., 2020). For example, Dhiman et al. (2018) used the spotted hyena optimization algorithm to solve the nonlinear economic dispatch problem of thermal power units and compared the effects of considering or not considering transmission loss, valve point effect and multiple fuel supply on minimizing the fuel cost of the units. Faced with the uncertainty of distributed energy output power in the economic dispatch model with virtual power plant, Huang et al. (2016) used the probability function in interval optimization to transform the model into a deterministic model for a reasonable prediction of distributed energy power and load demand for convenient solution, which helps to reduce the difficulty of economic dispatch, but the probability of interval is hard to determine. Xie et al. (2018) proposed an economic dispatch model based on multidisciplinary collaborative optimization with the objective of optimizing the energy cost of thermal power units. The study established a model based on the stochastic and fluctuating nature of wind power to optimize the grid dispatch problem under wind power integration by analyzing the prediction error of decoupled wind power scenarios. While most studies are based on day-ahead economic dispatch, there are also scholars who conduct real-time dispatched of units. Soroudi et al. (2017) proposed a stochastic real-time dispatched model to solve the dynamic economic dispatch problem by introducing the optimal conditional decomposition approach to address the rapidity of real-time dispatched. Reddy and Bijwe (2015) introduced dynamic variable cost for real-time dispatch to improve system economy, but frequent adjustment based on cost is not conducive to system stability. The single objective of economy cannot be considered only, and the environmental issues closely related to economy also need to attract the attention with the deepening research on power grid optimization.

The power generation mode has changed from pure thermal power generation to the coexistence of multiple generation such as thermal power unit, wind turbine and photovoltaic device with the deepening of research, and the research on power system unit dispatch has gradually developed from considering a single economic goal to considering economic, environmental, operational stability and other multi-objective directions. The technology for solving HDEED problems can be divided into mathematical methods and artificial intelligence methods. Mathematical methods include Lagrangian relaxation(Mahdi et al., 2019), linear programming, etc. Where, Espinosa et al. (2017) used mixed integer linear programming to solve the economic dispatch problem. CO<sub>2</sub> emissions are used as constraint and Coincplex is used to allocate generation power to thermal units within 24 hours. Nemati et al. (2018) used mixed integer linear programming through optimizer to deal with the constraints between network topologies through optimizers. Mathematical methods can be used to deal with simple EED problems, but with the increase of data and constraints, traditional mathematical methods are no longer enough to solve complex HDEED problems. Along with the development of computer technology, machine learning methods have been well used. Such

as particle swarm algorithm (Alshammari et al., 2020), artificial neural networks(Wang et al., 2021), genetic algorithm(Ganjefar and Tofighi, 2011), differential evolution algorithm(Basu, 2011), and mothballing algorithm(Hazra and Roy, 2020). In addition, Wang et al. (2021)proposed a recurrent neural network algorithm to solve the HDEED problem, which reduced randomness by strictly following the corresponding constraints at each time. Ma et al. (2018) used an improved global artificial bee colony algorithm to speed up the convergence of the algorithm to solve the HDEED problem, but lacked measures to prevent the algorithm from falling into local optimum. Chinnadurrai and Victoire (2020) proposed a non-dominated sorting crisscross optimization algorithm for global convergence and avoid premature convergence to maximize the utilization of wind power while optimizing operating cost and pollutant emission, and achieve better results in large, medium and small three-scale systems.

In addition to considering the wind and photovoltaic with large volatility, many studies have conducted more extensive research on HDEED according to the needs of different users or load environments. Liang et al. (2019) addressed the issue of economic emission by considering electric vehicles, and studied control strategies to achieve peak shaving and valley filling by using electric vehicles and showed that additional investment in power plant and pollutant emission could be reduced, but the use of electric vehicles for regulation devices lacked practicality. Yang et al. (2020) proposed a super-heuristic algorithm that enhance search diversity for solving the HDEED problem incorporating wind, photovoltaic and energy storage. However, too little research has been done on the energy storage component and it is difficult to see the role played by energy storage devices. Song et al. (2021)constructed a two-layer economic environment balance model integrating thermal power and natural gas, which increased the reliability of power supply while using thermal and natural gas power generation to serve different users. Scenario analysis method is used to determine the operation plan and power-to-gas plant was used to improve the utilization of wind power.

The construction of new microgrid is combined cool, heat and electricity and shows that prior studies tend to address the HDEED issue with the objective of improving the economic benefits of the electricity operators and reducing pollutant emissions. However, few studies use energy storage devices to mitigate the impact of renewable energy prediction errors to ensure the stability of power grid operation.

### **3. System framework for solving HDEED problem by using IMA algorithm**

This section establishes a dispatch model that considers both economic and environmental protection. Different from most studies that only consider the minimum optimization target, by analyzing the volatility of renewable energy output under actual conditions, innovatively proposed a distribution strategy for renewable energy that optimizes the economic and environmental goals while ensuring the stable output of renewable energy. Secondly, an optimization algorithm with better effect on the model is selected and improved in solving the problem of HDEED. Finally, the membership function is introduced to select the best solution in the solution set obtained by the optimization algorithm. The following content describes these parts.

#### ***3.1. Multi-objective optimization model for electricity system***

This study uses the power generated by thermal power units, wind turbines, photovoltaic device and energy storage power station as the grid power. In optimizing dispatch strategy, it is necessary to optimize the output of thermal power units and renewable energy respectively and consider more constraints.

##### ***3.1.1. Objective functions***

In order to achieve the optimal balance between economic and environmental, the goal of HDEED is to minimize operating cost and pollutant emission.

### Objective 1. Minimize operation cost

Reducing operation cost is conducive to improving production efficiency and increasing the revenue of system operator. The sum cost of system includes the power generation cost of thermal power units, wind turbines and photovoltaic device, and the energy storage cost of energy storage power station. As the thermal power units with highest power generation, the valve point effect should also be considered (Nazari-Heris et al., 2018). Considering the nonconvex optimization problem, a sine function is added to the cost function of units, and the cost function expression of the thermal power units considering the valve point effect is as follows:

$$f_{1c} = \sum_{t=1}^T \sum_{i=1}^N \left\{ (a_i P_{i,t}^2 + b_i P_{i,t} + c_i) + \left| g_i \sin \left[ h_i (P_{i,t} - P_i^{\min}) \right] \right| \right\} \quad (1)$$

Where  $f_{1c}$  represents the cost of generating electricity for thermal power units;  $N$  is the number of thermal power units;  $P_{i,t}$  represents the generating power of the  $i$ th thermal power unit at the  $t$ th hour;  $a_i$ ,  $b_i$ , and  $c_i$  are the fuel cost coefficients of thermal power units;  $T$  is the total time of a dispatch period;  $g_i$  and  $h_i$  are the valve point impact coefficients of units;  $P_i^{\min}$  represents the minimum power limit of  $i$ th units.

At the same time, considering the higher manufacturing cost and depreciation cost of wind turbines, photovoltaic device and energy storage power station, the cost of wind, photovoltaic and energy storage devices after conversion is shown in equation (2):

$$f_{2c} = \sum_{t=1}^T \left( \sum_{i=1}^J c_w P_{i,t}^w + \sum_{i=1}^K c_{pv} P_{i,t}^{pv} + c_{bat} |P_t^{bat}| \right) \quad (2)$$

Where  $c_w$ ,  $c_{pv}$ ,  $c_{bat}$  are the cost coefficients of wind, photovoltaic and energy storage devices;  $J$  and  $K$  represent the number of wind turbines and photovoltaic devices respectively;  $P_{i,t}^w$ ,  $P_{i,t}^{pv}$  represent the dispatched power of the  $i$ th wind turbine and photovoltaic device at time  $t$ ; and  $P_t^{bat}$  represents the output or input power of the energy storage power station at time  $t$ .

Therefore, the total cost of the HDEED system is shown in equation (3):

$$\min F_{\text{cost}} = f_{1c} + f_{2c} \quad (3)$$

### Objective 2. Minimize Pollutant emission

Thermal power units produce large amounts of carbon dioxide and other polluting gases, which are harmful to the environment. Wind and photovoltaic generation as an environmentally friendly renewable energy generation method, increase the corresponding proportion of power generation can reduce pollutant emission, and pollutant emission from wind and photovoltaic installations can be ignored at the same time (Li et al., 2021a). In this study, the minimum value of pollutant emission is determined by analyzing the relationship between the power of thermal power units. The corresponding emission formula can be expressed as equation (4).

$$\min F_{\text{emi}} = \sum_{t=1}^T \sum_{i=1}^n [o_i + p_i P_{i,t} + q_i P_{i,t}^2 + \theta_i \exp(\varphi_i P_{i,t})] \quad (4)$$

Where  $o_i$ ,  $p_i$ ,  $q_i$ ,  $\theta_i$  and  $\varphi_i$  represent the pollutant emission coefficients of the  $i$ th Thermal power unit.

This study uses a weighted approach to transform multi-objective into a single-goal optimization solution. Obtains a set of Pareto solution sets by changing the weight coefficient,

and finally gets a compromise solution of multiple goals by the subordinate function. The objective function is as follows:

$$\min F = \omega F_{\text{cost}} + (1-\omega)F_{\text{emi}} \quad (5)$$

Where  $F$  represents the objective function combined with weight; The value of weight  $\omega$  changes in the range of 0-1. Since the operating cost and pollutant emission of the two objectives are contradictory, the value of  $\omega$  is used to change the optimal proportion of operating cost and pollutant emission to determine the compromise solution.

As weight formula that transforms multiple objectives into a single objective function for optimization, some problems of equation (5) need to be improved are found in this study. That is, when the value of fitness is calculated in equation (5) by changing the weight coefficient  $\omega$  to obtain a set of Pareto solutions, the change of the weight coefficient  $\omega$  will not have a better effect on the choice of compromise solution of the objective function if operation cost and pollutant emission are of different magnitudes. Therefore, the objective function is modified to introduce proportional coefficient  $Q$  into the fitness function, and the value of  $Q$  depends on the magnitude difference between the different objectives. The modified objective function is as follows:

$$\min F = \omega F_{\text{cost}} + Q(1-\omega)F_{\text{emi}} \quad (6)$$

### 3.1.2. System constraints

The constraints of the entire system and each power generation module need to be considered in HDEED model.

#### (1) Power balance constrains of HDEED system

The operation of power transmission network needs to maintain the power balance between power generation and load at all times, otherwise it will affect the safety of the system and cause damage to the electrical equipment.

When the dispatched power of energy storage power station is greater than zero, the sum of output power of the thermal power units, wind turbines, photovoltaic device and energy storage power station should be equal to the total load and transmission loss of the system, otherwise the power of the thermal power units, wind turbines and photovoltaic device equal to load and transmission loss.

$$\begin{cases} \sum_{i=1}^N P_{i,t} + \sum_{i=1}^J P_{i,t}^w + \sum_{i=1}^K P_{i,t}^{pv} = P_t^{\text{load}} + P_t^{\text{loss}}, P_t^{\text{bat}} < 0 \\ \sum_{i=1}^N P_{i,t} + \sum_{i=1}^J P_{i,t}^w + \sum_{i=1}^K P_{i,t}^{pv} + P_t^{\text{bat}} = P_t^{\text{load}} + P_t^{\text{loss}}, P_t^{\text{bat}} > 0 \end{cases} \quad (7)$$

Where  $P_t^{\text{load}}$  represents the load power at time  $t$ ;  $P_t^{\text{loss}}$  represents the transmission loss at time  $t$ . The expression of transmission loss is as shown:

$$P_t^{\text{loss}} = \sum_{i=1}^N \sum_{j=1}^N P_{i,t} L_{i,j} P_{j,t} + \sum_{i=1}^N P_{i,t} L_i + L_o \quad (8)$$

Where  $L_{i,j}$ ,  $L_i$  and  $L_o$  represent transmission loss coefficients.

#### (2) Power constraints of thermal power units

The power generated from thermal power units in HDEED system must not exceed the power limit in equation (9).

$$P_i^{\text{min}} \leq P_i \leq P_i^{\text{max}} \quad (9)$$

Where  $P_i^{\text{min}}$  and  $P_i^{\text{max}}$  represent the minimum and maximum power of  $i_{\text{th}}$  unit.

A rapid increase or decrease in output power will damage the generator, so the output power is controlled within a certain range by setting the limits of power change. The constraints are illustrated as follows:

$$\begin{cases} P_{i,t} - P_{i,t-1} \leq P_i^U, & \text{if } P_{i,t} > P_{i,t-1} \\ P_{i,t-1} - P_{i,t} \leq P_i^D, & \text{if } P_{i,t} < P_{i,t-1} \end{cases} \quad (10)$$

Where  $P_i^U$  and  $P_i^D$  are rise and fall boundaries of power change of  $i^{\text{th}}$  unit.

### (3) Power constraints of wind and photovoltaic generation

Wind and photovoltaic, as renewable energy sources, are greatly affected by the environment during power generation and need to be dispatched within the scope of the forecast output.

$$0 \leq P_{i,t}^w \leq P_{t,\max}^w \quad (11)$$

$$0 \leq P_{i,t}^{pv} \leq P_{t,\max}^{pv} \quad (12)$$

Where  $P_{t,\max}^w$  and  $P_{t,\max}^{pv}$  respectively represent the maximum output power of wind and photovoltaic device at time  $t$ .

### (4) Charge-discharge power and energy balance constraints of energy storage power station

$$-P_D^{bat} \leq P_t^{bat} \leq P_R^{bat} \quad (13)$$

Where  $P_R^{bat}$  is the maximum discharge power of the energy storage power station;  $P_D^{bat}$  is the maximum charge power;  $P_t^{bat}$  is the charge or discharge power dispatched by energy storage power station at time  $t$ ; The energy storage power station discharges when  $P_t^{bat}$  is greater than zero and charges when it is less than zero.

As the energy storage power station has a certain capacity, the state of energy storage at each moment is limited by the previous state and the phenomenon of excessive charging or discharging needs to be prevented (Gaspar et al., 2021). Therefore, an energy constraint is added to the energy storage power station, as follows:

$$\begin{cases} E_{t+1} = E_t - \eta^{bat} P_t^{bat}, & P_t^{bat} < 0 \\ E_{t+1} = E_t - \frac{P_t^{bat}}{\gamma^{bat}}, & P_t^{bat} > 0 \end{cases} \quad (14)$$

$$0 \leq E_t \leq E_{\max} \quad (15)$$

Where  $E_t$  and  $E_{t+1}$  are the electricity quantity of the energy storage power station at time  $t$  and the next time respectively; The efficiency of both charging and discharging of the energy storage power station are  $\eta^{bat}$ ;  $E_{\max}$  represents the maximum capacity of the energy storage power station, and the electricity quantity at each time should be within the bounded range.

To prevent damage to the energy storage system, the storage power station also needs to meet the requirement that the charge and discharge quantity are equal in one or more cycles. In the study, the charge and discharge quantity of energy storage power station is set to be equal in a dispatch cycle, as follows:

$$\sum_{t=1}^T P_t^{bat} \approx 0 \quad (16)$$

#### 3.1.3. Wind-photovoltaic stability output strategy

The dispatch power of wind and photovoltaic generation does not subject to other constraints except taking the forecast power of wind and photovoltaic as maximum reference power in most studies on the optimal dispatch of multiple energy sources including wind, solar and thermal energy. If the time-of-use electricity price is not considered, the energy storage device as a peak-shaving and valley-filling tool will makes the output power of wind and photovoltaic to the grid is large in optimization due to the high manufacturing and operation costs of the energy storage device, which makes the energy storage device does not play a better role.



Where  $X^l$  represents the male population after the  $i_{th}$  iteration;  $x_{i,j}^l$  is the position of  $i_{th}$  individual in  $j_{th}$  dimension after the  $l_{th}$  iteration;  $N$  is the size of the population, and  $D$  is the dimension of the problem to be solved. The position matrix of female population is as follows:

$$Y^l = \begin{bmatrix} y_{1,1}^l & y_{1,2}^l & \dots & y_{1,D}^l \\ y_{2,1}^l & y_{2,2}^l & \dots & y_{2,D}^l \\ \dots & \dots & \dots & \dots \\ y_{N,1}^l & y_{N,2}^l & \dots & y_{N,D}^l \end{bmatrix} \quad (18)$$

Where  $Y^l$  represents the female population after the  $l_{th}$  iteration, both the female and male mayfly populations have the same size are set to  $N$ .

The objective function is regarded as the fitness function of the population in the process of solving HDEED problem. The fitness matrix of male population can be obtained as follows:

$$Fit_{me}^l = [fit_1^l, fit_2^l, \dots, fit_N^l] \quad (19)$$

Where  $fit_N^l$  is the fitness corresponding to the  $N_{th}$  male mayfly in the  $i_{th}$  iteration. In the same way, the fitness matrix corresponding to the female mayfly population can be obtained as follows:

$$Fit_{fe}^l = [fit_1^l, fit_2^l, \dots, fit_N^l] \quad (20)$$

Where  $Fit_{fe}^l$  is the fitness matrix of female mayfly population;  $fit_N^l$  is the fitness corresponding to the  $N_{th}$  female mayfly in the  $i_{th}$  iteration.

## (2) Position update strategy of mayfly

Male mayflies update their position by jumping near the water surface, that is, adding the unit speed of the mayfly at the current position:

$$x_i^{l+1} = x_i^l + v_i^{l+1} \quad (21)$$

Male mayflies have a group character and does not have a large moving speed. The position update formula of male mayflies is described as follows:

$$\begin{cases} v_i^{l+1} = v_i^l + fl * e & f(x_i) < f(g_{best}) \\ v_i^{l+1} = v_i^l + k_1 e^{-\beta r^2} (p_{best} - x_i^l) + k_2 e^{-\beta r^2} (g_{best} - x_i^l) & f(x_i) > f(g_{best}) \end{cases} \quad (22)$$

Where  $v_i^l$  is the velocity of  $i_{th}$  male mayfly in  $l_{th}$  iteration;  $x_i^l$  is the position of  $i_{th}$  male mayfly in the  $l_{th}$  iteration;  $k_1$  and  $k_2$  are positive attraction coefficients;  $rp$  is the distance between local optimal position and  $i_{th}$  male mayfly in the current iteration;  $rg$  is the distance between global optimal position and  $i_{th}$  male mayfly;  $p_{best}$  and  $g_{best}$  are the local optimal position and the global optimal position respectively.

Unlike male mayflies, female mayfly does not congregate in fixed place, but are attracted by male mayfly, and moving towards male mayfly positions. Assuming that the best female mayfly will move towards the best male mayfly position, and the formula for the position and speed of female mayfly are as shown:

$$y_i^{l+1} = y_i^l + v_i^{l+1} \quad (23)$$

$$v_i^{l+1} = \begin{cases} v_i^l + fl * e & f(y_i) < f(x_i) \\ v_i^l + k_3 e^{-\beta r^2} (x_i^l - y_i^l) & f(y_i) > f(x_i) \end{cases} \quad (24)$$

Where  $y_i^{l+1}$  and  $v_i^{l+1}$  are the position and speed of the  $i_{th}$  female mayfly after the update;  $fl$  is the random walk coefficient of the female mayfly;  $e$  is a random number between -1 and

1 that changes with the number of iterations;  $k_3$  is a fixed attraction coefficient of female mayflies; and  $r$  is the distance between the  $i_{th}$  male mayfly and the female mayfly.

### (3) Mating produces offspring

Most animals and plants follow the principle of survival of the fittest when mating. Assuming that mayflies are attracted to each other for mating according to their fitness. That is, the best adapted female and male will mate and produce a female and a male offspring. The results are as follows:

$$\begin{cases} new1 = q * x_i + (1 - q) * y_i \\ new2 = (1 - q) * x_i + q * y_i \end{cases} \quad (25)$$

Where  $q$  is a random number from -1 to 1 with the same dimension as  $x$  and  $y$ ;  $x_1$  and  $y_1$  are the  $i_{th}$  male and female mayfly sorted by fitness;  $new1$  and  $new2$  are offspring of the generation.

### 3.2.2 Improved mayfly optimization algorithm

#### (1) Chaos map initialization population

To find optimal solution of population faster and maintain the randomness of the initial population as much as possible, logistic chaotic mapping is introduced to improve the initialization method of MA algorithm, which is expressed as follows:

$$x_i = z_i * (ub - lb) + lb \quad (26)$$

Where  $x_i$  represents the position of the  $i_{th}$  male mayfly after chaos initialization;  $ub$  and  $lb$  represent the upper and lower limits of the mayfly position;  $z_i$  is a chaotic sequence with the same dimension as  $x_i$ . Generate other  $z$  through the logistic mapping formula and a  $z_1$  vector randomly generated between 0-1, as shown:

$$z_i = \mu * z_{i-1} * (1 - z_{i-1}) \quad (27)$$

Where  $\mu$  is an adjustable parameter, and all values of  $z$  can be chaotic when the value of  $\mu$  is 4. The initial position of the female mayfly is also available:

$$y_i = z_i * (ub - lb) + lb \quad (28)$$

#### (2) Adaptive weight factor

The introduction of adaptive weight factor in the mayfly speed update can enhance the global or local search ability. The larger weight in the early stage is conducive to the global search. The search range is determined in the final stage, which can reduce the adaptive factor and find the optimal solution within a certain range. The square value of the sine function can be used to keep the larger adaptive factor in the initial stage and the smaller adaptive factor in the final stage for a long time. The expression of the adaptive factor  $w$  is as follows:

$$w^l = w_{\max} - (w_{\max} - w_{\min}) * \sin\left(\frac{l * \pi}{2L}\right)^2 \quad (29)$$

Where  $w^l$  represents the adaptive factor at the  $l_{th}$  iteration;  $L$  represents the maximum value of iterations.  $w_{\max}$  represents the maximum value of the adaptive factor and the value is 1;  $w_{\min}$  represents the minimum value of the adaptive factor and the value is 0.5.

To show the effect of adaptive weight factor, several common weights are used as comparisons. Figure 2 shows the iterative curves of multiple weight factors.

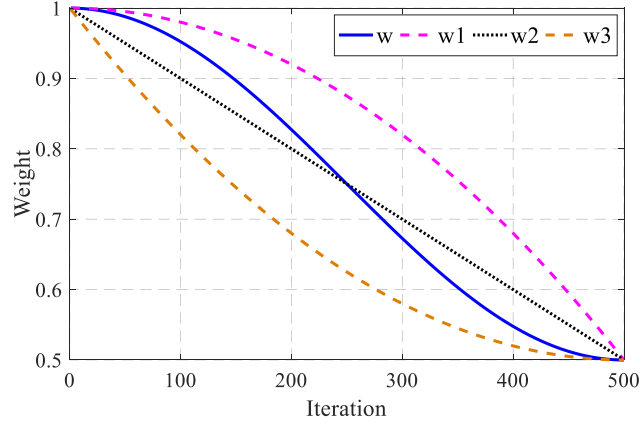


**Figure 2.** Adaptive factor

Where the blue curve is the adaptive weight factor  $w$  proposed in this study, and the remaining  $w1$ ,  $w2$  and  $w3$  represent several commonly used weight factors respectively (Arasomwan and Adewumi, 2013; Shi and Eberhart, 1998). The result shows that the adaptive weight factor used in this study can improve the optimization effect of IMA algorithm by combining larger values of  $w1$  in early iterations and smaller values of  $w3$  in late iterations.

The update formula of the male mayfly speed after adding the adaptive weight factor is as follows:

$$v_i^{l+1} = w^l v_i^l + k_1 e^{-\beta r p^2} (p_{best} - x_i^l) + k_2 e^{-\beta r g^2} (g_{best} - x_i^l) \quad (30)$$

The speed update formula for female is as follows:

$$v_i^{l+1} = \begin{cases} w^l v_i^l + fl * e & f(y_i) < f(x_i) \\ w^l v_i^l + k_3 e^{-\beta r^2} (x_i^l - y_i^l) & f(y_i) > f(x_i) \end{cases} \quad (31)$$

### (3) Offspring mutation

Among the offspring of mayfly, the best male and female individual mate to produce offspring, this makes it easy for algorithm to fall into local optimization during iteration. Mutation operation is added to the offspring of mayfly to improve the global search ability. The mutation formula is as follows:

$$mutnew = new + \psi \quad (32)$$

Where  $mutnew$  represents the offspring after mutation;  $new$  represents the offspring after mating; and  $\psi$  is the value of mutation.

The method of calculating the mutation value is improved to reduce the invalid mutation as much as possible and let the offspring mutate within the search range. Increase the mutation value in the early stage and mutate as many times as possible in the global scope. Correspondingly reduce the mutation value in the later stage to improve the efficiency of the mutation. The improved mutation formula is expressed as shown:

$$\begin{cases} \psi = 0, & \text{if } \delta = 0 \\ \psi = unifrnd(-1,1) * (1 - 0.5 * l / L) * g_{best} / 2, & \text{if } \delta = 1 \end{cases} \quad (33)$$

Where  $unifrnd(-1,1)$  represents a random number between -1 and 1;  $\delta$  is the mutation factor, which is affected by the probability of mutation.

### (4) Worst position update strategy

Among the new population generated after crossover and mutation, a certain number of mayflies with the worst positions will update their positions refer to the best position mayflies,

which is beneficial to improve the local search ability of mayflies. Set the worst mayfly to update by reference to the position of three mayflies, as follows:

$$\begin{cases} x_{N-i}^{l+1} = \frac{x_i^l + x_{i+1}^l + x_{i+2}^l}{3} \\ y_{N-i}^{l+1} = \frac{y_i^l + y_{i+1}^l + y_{i+2}^l}{3} \end{cases} \quad (34)$$

where  $x_{N-i}^{l+1}$  and  $y_{N-i}^{l+1}$  represent the male and female individuals after the worst mayfly position is updated.

### 2.3. Membership function

After obtaining a set of Pareto solutions of operating cost and pollutant emission under different weight coefficients by using equation (6), the membership function is introduced to calculate the satisfaction of Pareto solution sets (Li et al., 2021b). The main steps are as follows:

(1) The satisfaction degree of each dimension of Pareto solution is calculated:

$$\phi_{k,i} = \begin{cases} 1 & f_{k,i} \leq f_k^{\min} \\ \frac{f_k^{\max} - f_{k,i}}{f_k^{\max} - f_k^{\min}} & f_k^{\min} < f_{k,i} < f_k^{\max} \\ 0 & f_{k,i} \geq f_k^{\max} \end{cases} \quad (35)$$

Where  $\phi_{k,i}$  represents the satisfaction of  $k$ th dimension in  $i$ th solution;  $f_k^{\max}$  and  $f_k^{\min}$  represent the upper and lower bounds of the  $k$ th dimension.

(2) The comprehensive satisfaction of each solution is calculated:

$$\phi_i = \frac{\sum_{k=1}^n \phi_{k,i}}{\sum_{i=1}^l \sum_{k=1}^n \phi_{k,i}} \quad (36)$$

Where  $n$  is the number of dimensions, which represents the objective of cost and emission in this study.

(3) The satisfaction of Pareto solution set is comprehensively analyzed to choose the best compromise solution.

### 2.4 Flow framework for solving HDEED problem

Figure3 shows the flow framework for optimizing HDEED problem by using wind-photovoltaic stability output strategy and IMA algorithm. The model interacts with two optimization levels of the wind and photovoltaic power optimization level and the IMA optimization level, and ultimately combines the membership function to calculate pareto solution set through equation (35) and equation (36) to obtain the compromise solution.

In practical application, the wind and photovoltaic power optimization level is closely integrated with the IMA optimization level. Based on the analysis of the predicted wind and photovoltaic power within a cycle, the dispatch power of the wind turbines, photovoltaic device and energy storage power station connected to the transmission network is then determined and the result of dispatch power is transmitted to the IMA optimization level. The IMA optimization level combines the load demand and the power from the wind and photovoltaic power optimization level to optimize the power of thermal power units and obtains pareto solution set by changing the weight coefficient  $\omega$ . The specific process of IMA optimization level in HDEED model is as follows:

(1) The parameters and constraints of load, thermal power units, wind turbines, photovoltaic device and energy storage power station are received, the weight coefficient  $\omega$  and

proportional coefficient  $Q$  are determined, and the IMA algorithm starts to run.

- (2) Initialize the parameters of IMA algorithm and evaluate the fitness value of population to select the local and global optimal solutions.
- (3) Update the position and velocity of male and female mayfly, then the fitness value of each mayfly is evaluated by the equation (6), and the global and local optimum are updated.
- (4) Crossover and mutation operations are carried out to produce a certain number of offspring, and the offspring and parents are sorted according to fitness values to produce a new generation of female and male populations with number  $N$ .
- (5) Update the adaptive weight factor with equation (29) and other coefficients.
- (6) Judge the termination condition, and output the optimal solution obtained by the IMA algorithm if the condition is met.
- (7) The weight coefficient  $\omega$  of equation (6) is increased by 0.05 from 0 to 1 in order, and the IMA algorithm is repeated to obtain the pareto solution set and output.

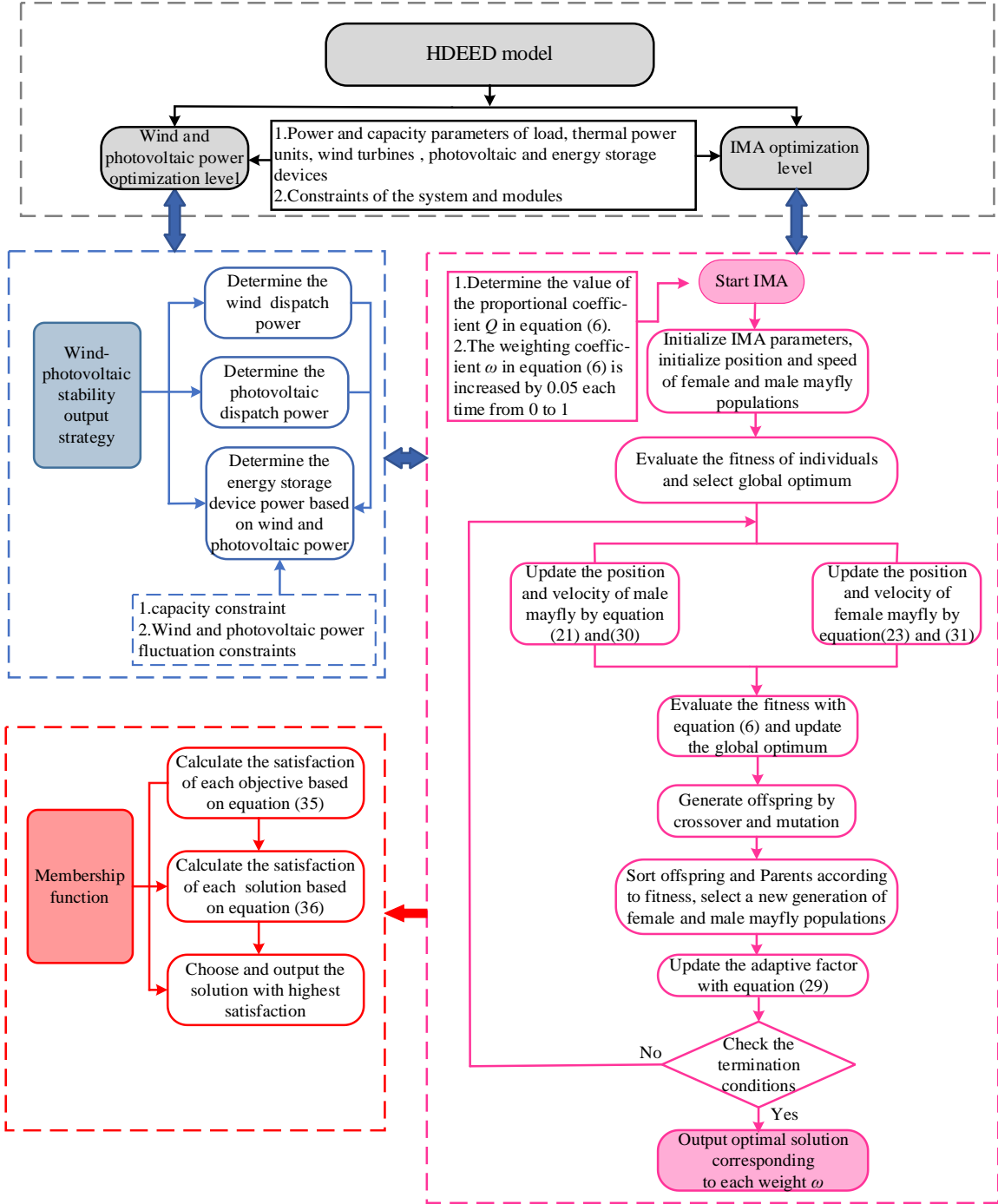


**Figure 3.** Flow framework of the power system

#### 4. Performance analysis of the proposed IMA algorithm

Using only one type of benchmark function cannot show the characteristics of the algorithm. Therefore, this study introduces four different types of benchmark functions to verify the optimization ability of the improved algorithm. In test function,  $f_1$  and  $f_2$  represent the unimodal function, which can be used to test the convergence speed and accuracy of the algorithm.  $f_3$  represents multimodal function that can effectively test the algorithm out of the local optimum.  $f_4$  is a composite test function to verify the convergence speed of the algorithm. The four benchmark functions are shown in Table 1.

The PSO (Mohammadian et al., 2018), MFO (Mirjalili, 2015) and MA algorithms are

selected to compare to verify the convergence performance of the improved MA algorithm with same amount of iterations. The number of iterations and population size are 1000 and 30 respectively, and other parameters of each algorithm are shown in Table 2.

**Table 1.** Benchmark function

Function	Range	Dim	Theoretical minimum
$f_1(x) = \sum_{i=1}^n x_i^2$	[-100,100]	10	0
$f_2(x) = \sum_{i=1}^n  x_i  + \prod_{i=1}^n  x_i $	[-10,10]	30	0
$f_3(x) = \sum_{i=1}^n [x_i^2 - 10\cos(2\pi x_i) + 10]$	[-5.12,5.12]	30	0
$f_4(x) = \sum_{i=1}^{11} \left[ a_i - \frac{x_i(b_i^2 + b_1 x_2)}{b_i^2 + b_1 x_3 + x_4} \right]^2$	[-2,5]	4	0

**Table 2.** Algorithm parameters

Algorithm	parameters
PSO	$c1=1, c2=2, w=0.5$
MFO	$b=1$
MA	$a1=1, a2=1.5, a3=1.5, fl=0.1$
IMA	$g_{max}=1, g_{min}=0.5, a1=1, a2=1.5, a3=1.5, fl=0.1, d=0.1$

In PSO algorithm,  $c1$  and  $c2$  are learning factors and  $w$  is inertia weight.  $b$  is the spiral degree of the MFO algorithm. In MA algorithm,  $a1$ ,  $a2$  and  $a3$  are positive attraction coefficients of the mayfly, and  $fl$  is the random flight coefficient. In IMA algorithm,  $g_{max}$  and  $g_{min}$  are the maximum and minimum weight coefficients associated with the speed of radon, and  $d$  is the dance coefficient. Each test function is run 20 times to improve the reliability of the results, and the average, standard deviation, optimal value, worst value, and number of results above the average are calculated. The test results are shown in Table 3, and the iterative curve is obtained when the algorithm gets the optimal value by running it repeatedly, as shown in Figure 2. The experiment is run in MATLAB R2016b and based on Windows10 system Intel (R) Core (TM) i5-6200U CPU.

Table 3 illustrates the running results of the benchmark functions  $f_1$ ,  $f_2$ ,  $f_3$  and  $f_4$  on the four algorithms. The results show that IMA algorithm has better convergence speed and accuracy, with the largest number of solutions running 20 times above average and higher stability. Combined with Figure 4, in the unimodal function, the MA algorithm has obvious effects compared to PSO and MFO, and the IMA algorithm has better convergence speed and accuracy than original MA algorithm. In the multimodal function, the optimization effect of IMA algorithm is more prominent, and the optimal solution can reach 0. The IMA algorithm converges more quickly in the early stage and finds the largest number of solutions exceed the average for composite test functions.

From the iteration curves, thanks to the chaotic initialization method, the IMA algorithm converges fastest and requires the least number of iterations to find the optimal solution even though the value of the degree of adaptation is large at the initial moment. The use of mutation strategy, weight coefficient and the worst position update strategy enhances the optimization ability of IMA algorithm to find better results in terms of Average, Standard Deviation, best fitness and number.

Konstantinos et al. proposed an improved MA algorithm while proposing the original MA algorithm. By running the four test functions  $f_1(x)$ ,  $f_2(x)$ ,  $f_3(x)$  and  $f_4(x)$  under the same conditions, the average values were obtained as 1.1658e-80, 1.4361e-10, 7.1639, 3.7181e-04 respectively, while the average values obtained by the IMA algorithm were 3.0022e-105, 6.1588e-25, 4.3778, 3.5327e-04, it is obvious that IMA algorithm has better optimization ability than the improved algorithm proposed by Konstantinos and can be used for the study of HDEED problem.

**Table 3.** Statistical results of the benchmark function

Function	Algorithm	Average	Std	Best fitness	Worst fitness	number
$f_1(x)$	PSO	0.1375	0.3129	1.0795e-06	1.4058	16
	MFO	2.2422e-30	6.4137e-30	6.1587e-34	2.8100e-29	17
	MA	5.6138e-75	1.3972e-74	8.0155e-80	5.8431e-74	16
	IMA	3.0022e-105	9.5307e-105	3.2943e-114	3.9959e-104	18
$f_2(x)$	PSO	20.7209	3.9115	14.2147	28.0578	11
	MFO	34.0013	22.5701	8.1190e-04	70.0000	10
	MA	7.1557e-11	8.3120e-11	3.6144e-12	3.8077e-10	14
	IMA	6.1588e-25	1.2941e-24	1.4322e-26	5.7531e-24	17
$f_3(x)$	PSO	117.4759	27.0250	76.8657	188.8145	11
	MFO	151.8229	39.5464	79.5966	221.1638	11
	MA	78.0045	25.6409	34.8235	136.3087	11
	IMA	4.3778	3.9720	0	13.9294	13
$f_4(x)$	PSO	7.0514e-04	3.3347e-04	3.0749e-04	0.00103	8
	MFO	0.0010	4.7881e-04	5.2226e-04	0.0022	13
	MA	0.0011	0.0025	3.0749e-04	0.0109	17
	IMA	3.5327e-04	2.0475e-04	3.0749e-04	0.0012	19

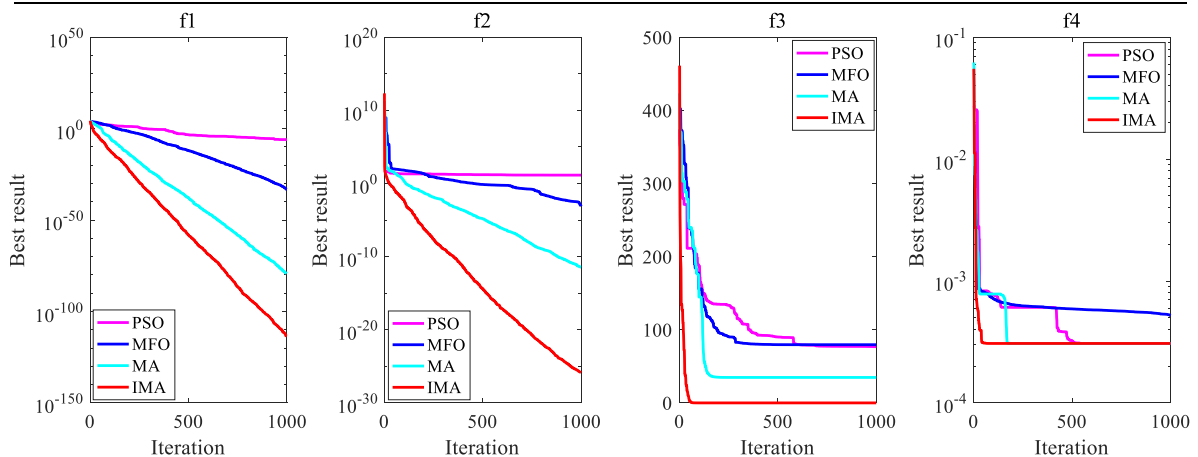


**Figure 4.** Comparison of algorithm iteration curves

## 5. Case study

In this section, two Systems are used to verify the effectiveness and practicability of the IMA algorithm and wind-photovoltaic output strategy. System 1 includes 5 thermal power

units, 2 wind turbines, 1 photovoltaic device and 1 energy storage device; System 2 includes 10 thermal power units, 3 wind turbines, 2 photovoltaic devices and 1 energy storage device. The established model and algorithm are combined to verify the performance of IMA algorithm, and then the IMA algorithm is used to analyze the wind-photovoltaic output strategy. The power of wind turbine and photovoltaic device required for the study are referenced in Mohy-ud-din (2017) and (Ye et al., 2021). The load power curve used in the two Systems is shown in Figure 5 (Liu et al., 2021; Qian et al., 2020).

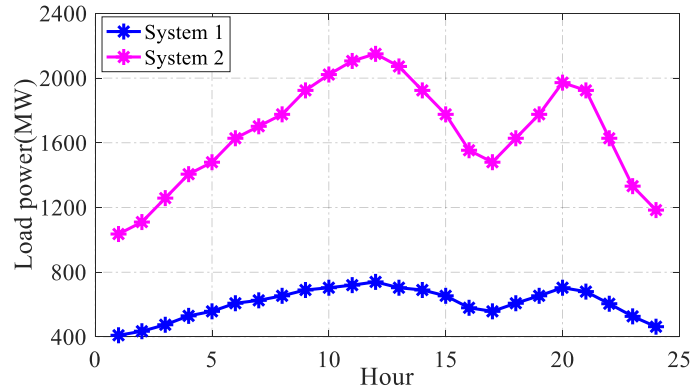


Figure 5. Load power in two Systems

### 5.1. System 1

The first part is the study of the improved algorithm on the HDEED problem, and the second part is the study of the introduction of wind-solar stability output strategy. The research of System 1 including 5 thermal power units is divided into two parts. The first part is the study of HDEED problem combination algorithm. The second part is the study of wind-photovoltaic stable output strategy. The energy storage devices could not be charged and discharged at the same time to facilitate the study.

#### 5.1.1. Discussion on IMA optimization algorithm in System 1

In solving the Pareto solution set, it is necessary to determine the value of proportional coefficient  $Q$  in order to achieve better results in optimization of the algorithm based on the fitness function (6). The cost and pollutant emission have the same order of magnitude by running IMA algorithm, so the value of  $Q$  is taken as 0. Next, the weight coefficient  $\omega$  in the fitness function is increased from 0 to 1 by 0.05 each time, and the Pareto solution set is obtained by iterating IMA algorithm 500 times each time. Then the compromise solution is calculated to obtain the corresponding weight coefficient  $\omega$  of 0.5. The Pareto solution set for cost and pollutant emission is shown in Figure 6.

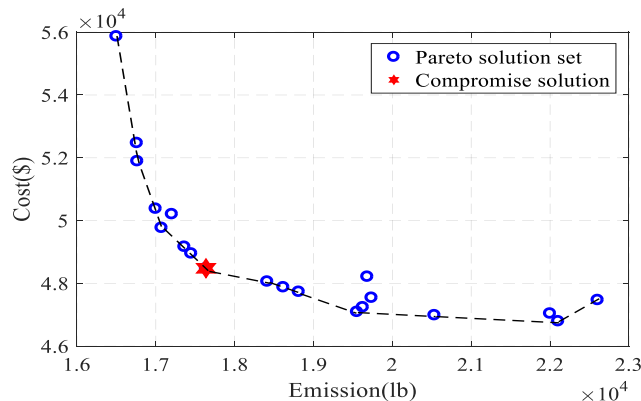


**Figure 6.** Pareto solution set in System 1

After combining the HDEED problem of System 1, the IMA algorithm is compared with MA algorithm, MFO algorithm and PSO algorithm, and the corresponding cost and pollutant emission are obtained as shown in Table 4. The operating cost and pollutant emission obtained by IMA algorithm are the smallest. Compared with MA algorithm, pollutant emission is reduced by 300lb, accounting for 1.68%; cost is reduced by 2023\$, accounting for 4.12%. Compared with the PSO and MFO algorithms with the high operation cost, the costs are reduced by 8387\$ and 7516\$ respectively, accounting for 15.14% and 13.21%. Pollutant emission are reduced by 1155lb and 1142lb respectively, accounting for 6.18% and 6.12%. The transmission loss obtained by different algorithms will not be particularly different, but the transmission loss corresponding to the thermal power is also small when System has a better search for the best result.

**Table 4.** Operating results of different algorithms for System 1

Algorithm	Cost (10 <sup>4</sup> ) (\$)	Emission (10 <sup>4</sup> ) (lb)	Loss (MW)
IMA	4.7020	1.7522	167.7475
MA	4.9043	1.7822	167.6299
MFO	5.4176	1.8664	170.9594
PSO	5.5407	1.8677	172.7660

Figure 7 shows the comparison of the operating cost and pollutant emission per hour of the four algorithms in System 1. The cost curve of IMA algorithm is close to that of MA algorithm, and the cost is much lower than that of PSO algorithm and MFO algorithm at most times. The operation cost of IMA and MA algorithms is much lower than that of other algorithms at the moment of 16.00-19.00 with lower load. While the emission curve obtained by different algorithms has different effects at each period. For the emission curve, the pollutant emission obtained by IMA algorithm are far lower than those obtained by MA, PSO and MFO algorithms at the first high load power, and the pollutant emission are slightly inferior to those obtained by MA algorithm at the later time, but the total emission in 24 hours is still the lowest. Therefore, IMA algorithm is lower than other algorithms in emission, and has achieved obvious results in operating cost.

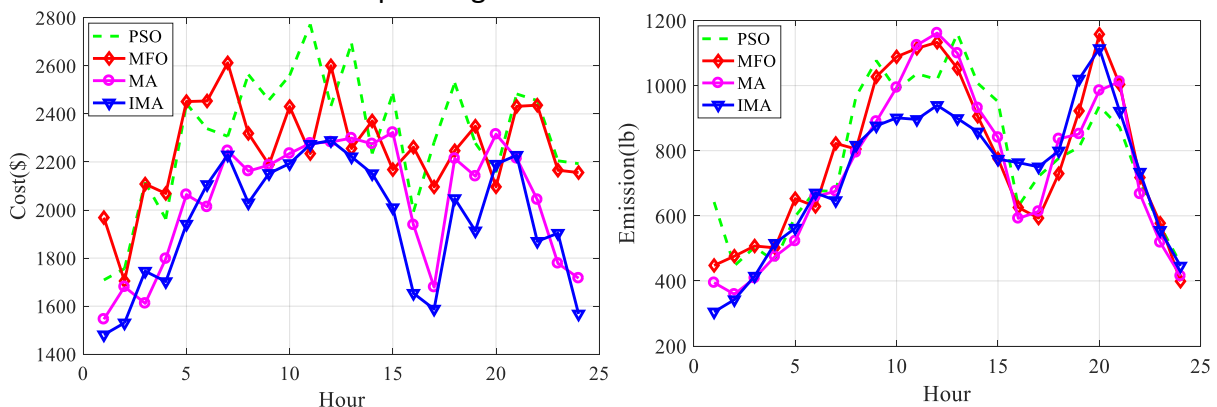


**Figure 7.** Objective curves of different algorithms for System 1

### 5.1.2. Discussion on wind and photovoltaic stability output strategy in System 1

The optimization ability of IMA algorithm is verified through the algorithm comparison, then the following discussion applies IMA algorithm to optimize HDEED problem in System 1

with wind-photovoltaic stable output strategy. To verify the effectiveness of the strategy, three models are used for comparative analysis.

Model 1: IMA algorithm with wind-photovoltaic stability output strategy.

Model 2: IMA algorithm without energy storage and wind-photovoltaic stability output strategy.

Model 3: IMA algorithm without wind-photovoltaic stability output strategy but with energy storage.

Energy storage discharges are also seen as part of renewable energy power due to charging surplus wind and photovoltaic power to energy storage power station. Figure 8 shows the total dispatched power of wind, photovoltaic and energy storage device of the three models in System 1. It shows that the power curve of Model 1 with the wind-photovoltaic stable output strategy is more stable in 24 hours. Even if the renewable energy power is small during the period of 8.00–10.00 and 17.00–20.00, a relatively stable total power is still obtained, indicating that the strong regulatory effect of the energy storage device. The power of Model 2 and Model 3 are unstable due to large fluctuation. The total renewable energy output for Model 1, Model 2 and Model 3 was calculated to be 956.41MW, 775.39MW and 934.70MW respectively in a cycle, with Model 1 having the highest renewable energy utilization of 956.41MW.

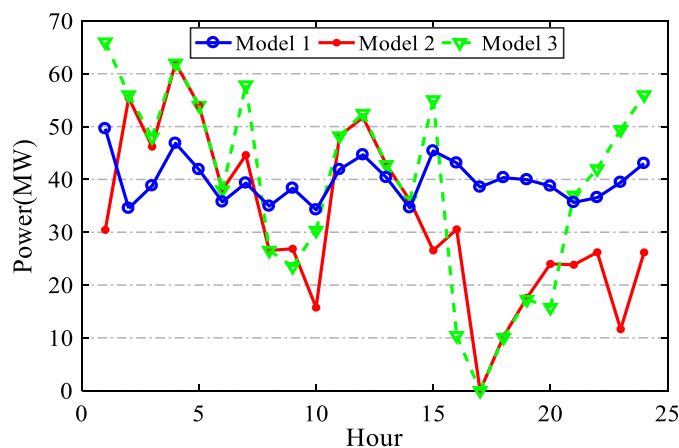
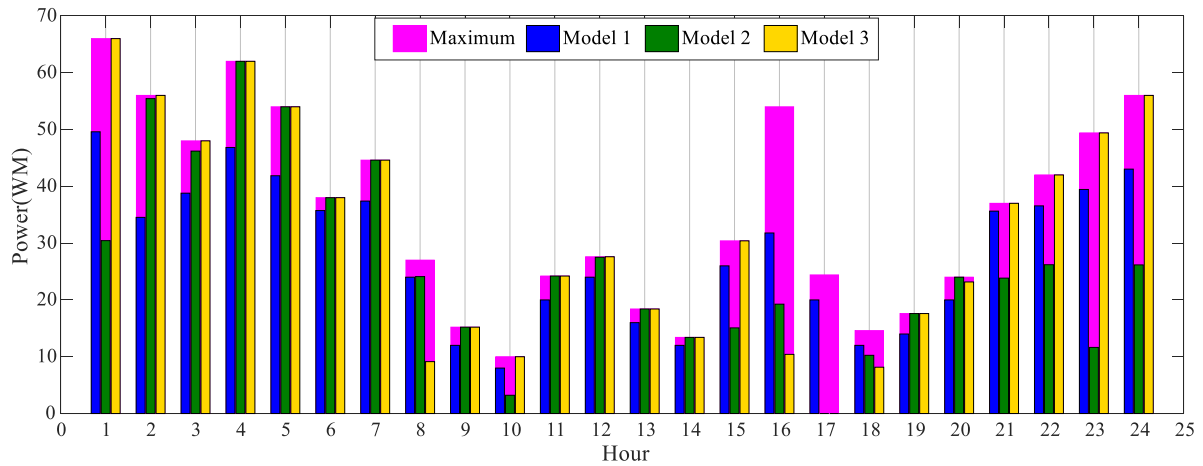


**Figure 8.** Renewable energy output of three models in System 1

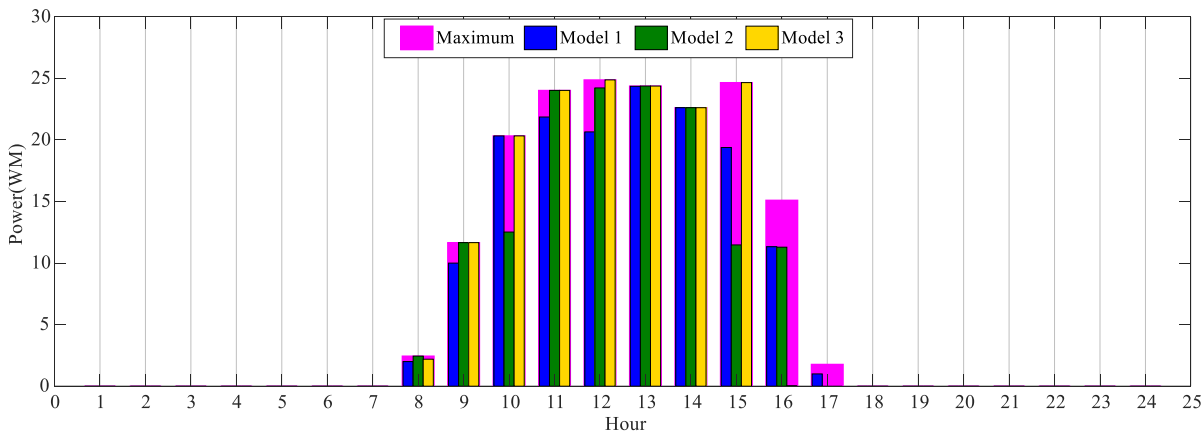
Table 5 shows the comparison of various parameters of the three models in System 1, including operating cost, pollutant emission, charge and discharge power and final power of energy storage device. Model 1 has a maximum operating cost of  $4.9591 \times 10^4$  \$ and a minimum pollutant emission of  $1.7009 \times 10^4$  lb. Model 2 has a reduced operating cost and an increased pollutant emission compared to other models as it does not need to consider the conflict between the cost of energy storage and the use of renewable energy. The discharge power is 28.50MW and the charge power is close to 0 in Model 3, even if the energy storage device is added, the wind power connected to the grid is not reduced when optimizing the operating cost and pollutant emission, which reduces the regulation effect of the energy storage device. According to the charge and discharge power in the Table 5, only Model 1 with control strategy can make full use of the effect of energy storage device, but it also causes a certain increase in cost due to the constant regulation of renewable energy generation by the energy storage device.

Figure 9 shows the comparison of wind and photovoltaic power of three models within 24 hours. At moments of 0.00–6.00 and 21.00–24.00, Model 1 reduces the wind power connected

to the grid, making the wind power lower than Model 3 without control strategy. In contrast, Model 2 greatly reduces the wind dispatched power at more times to reduce the value of fitness function, resulting in a large amount of wind abandonment. Due to the lack of control strategy, the dispatched power of Model 3 is directly equal to the forecasted output of wind and photovoltaic at most times. Although the renewable energy utilization rate of Model 3 in 24 hours is 934.70MW, it still does not make better use of renewable energy well at 8, 16 and 17 hours of wind power and photovoltaic. Only Model 1 can obtain the most stable and highest utilization of renewable energy dispatch.



(a) Comparison of wind power



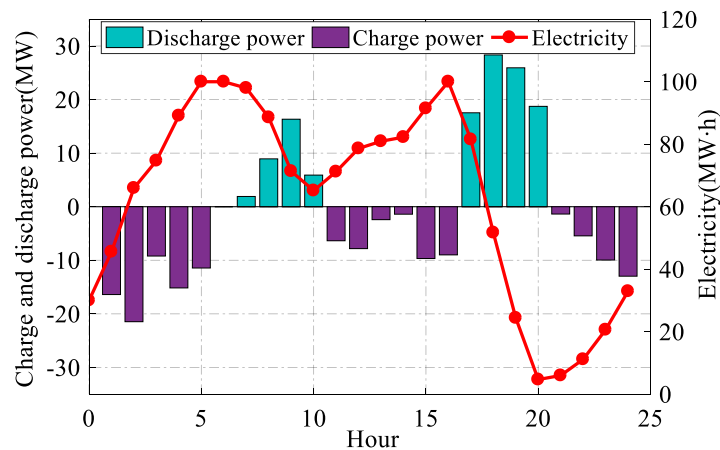
(b) Comparison of photovoltaic power

Figure 9. Different types of renewable energy output of three models for System 1

Table 5. Comparison of the results of three models for System 1

Model	Cost( $10^4$ )( \$)	Emission( $10^4$ )(l b)	Discharge power(MW)	Charge power(MW)	Electricity(MW · h)
Model 1	4.9591	1.7009	123.6059	-140.0956	32.94
Model 2	4.6731	1.7840	0	0	0
Model 3	4.7020	1.7522	28.5000	-1.24e-09	0

Table 6 shows the optimal dispatch power per hour for each unit of Model 1 in System 1. P1-P5 represent the dispatch power of five thermal power units, PW1-PW2 represent the dispatch power of two wind turbines, PV1 represents the dispatch power of photovoltaic device, P\_bat represents the dispatch power of the energy storage device, and E represents the hourly electricity of the energy storage power station. Figure 10 shows the optimal electricity and charge and discharge power of energy storage device of Model 1 in System 1. For ease of understanding make discharge power a positive value and charge power a negative value. The energy storage device uses wind power not connected to the grid to charge during the period when the wind power is high at 0.00-5.00 and 21.00-24.00. The power connected to the grid is also reduced to charge the energy storage power station during periods of high fluctuations in wind power from 11.00 to 16.00. The discharge of energy storage devices during the morning and evening peak of load demand is also conducive to reducing the peak load power applied to the thermal power units and maintaining the stable operation of the power grid. At the same time, the total charge power of energy storage device is 140.0956MW and the discharge power is 123.6059MW through reasonable dispatch, makes the charge and discharge power are relatively close in a dispatch cycle. The electricity is 30MW·h at 0th moment and 32.94MW·h at 24th moment, which is conducive to sustainability of the energy storage device dispatch. Combined with Table 5, Model 3 without control strategy has an electricity of 0 at 24th moment, which does not meet the requirements for sustainability.



**Figure 10.** Electricity and charge and discharge power of energy storage device for System 1

**Table 6.** The dispatch output of each power generation device of Model 1 for System 1

Hour	P1	P2	P3	P4	P5	PW1/2	PV1	E	P_bat
1.00	55.52	20.00	112.67	124.91	50.00	24.80	0.00	45.58	-16.40
2.00	75.00	40.39	112.67	124.91	50.00	17.27	0.00	65.98	-21.47
3.00	75.00	62.59	127.67	124.91	50.00	19.40	0.00	74.72	-9.21
4.00	75.00	92.59	112.67	124.91	82.84	23.42	0.00	89.13	-15.16
5.00	52.70	98.54	112.67	124.91	132.84	20.93	0.00	100.0	-11.44
6.00	75.00	98.54	140.81	124.91	139.76	17.86	0.00	100.0	0
7.00	75.00	98.54	112.67	167.90	139.76	18.70	0.00	97.99	1.91
8.00	75.00	98.54	175.00	209.82	68.85	12.00	2.00	88.58	8.94
9.00	75.00	98.54	158.35	209.82	118.85	6.00	10.00	71.38	16.34
10.00	75.00	98.54	156.01	209.82	139.76	4.00	20.33	65.17	5.90
11.00	66.93	97.52	175.00	208.34	139.57	10.00	21.87	71.20	-6.36

12.00	74.98	103.08	175.00	211.01	141.44	12.00	20.67	78.64	-7.82
13.00	47.32	95.40	175.00	206.76	148.12	8.00	24.36	80.94	-2.42
14.00	75.00	98.54	141.25	209.82	139.76	6.00	22.62	82.27	-1.40
15.00	64.26	92.32	111.75	209.12	139.72	13.00	19.39	91.46	-9.67
16.00	34.26	97.20	112.67	159.12	139.71	15.89	11.33	100.0	-8.99
17.00	49.18	98.54	112.67	124.91	139.76	10.00	1.00	81.54	17.54
18.00	27.15	90.82	112.00	200.16	144.98	6.00	0.00	51.71	28.34
19.00	61.28	98.54	112.67	209.82	139.76	7.00	0.00	24.41	25.94
20.00	75.00	69.85	175.00	212.14	142.44	10.00	0.00	4.68	18.74
21.00	75.00	98.54	129.97	209.82	139.76	17.81	0.00	5.98	-1.37
22.00	42.12	98.54	175.00	209.82	50.00	18.28	0.00	11.16	-5.44
23.00	21.89	98.54	112.67	209.82	50.00	19.72	0.00	20.61	-9.96
24.00	37.62	98.54	112.67	124.91	50.00	21.51	0.00	32.94	-12.98

Figure 11 shows the stacked bar chart of thermal power units dispatched power and renewable energy power of Model 1 in System 1. The uppermost curve represents the power required by the power grid every hour, that is, the sum power of load and network transmission loss. The top red part is the sum of wind, photovoltaic and energy storage discharge power, and the rest of each color represents the power dispatched by each thermal power unit. The output of each thermal power unit is more directly from the stacked bar chart. At the same time, according to the power curve of the power grid coincides with the top of the histogram, it revealed that the dynamic balance of power grid can be maintained at each time, which meets the power balance constraint of System 1.

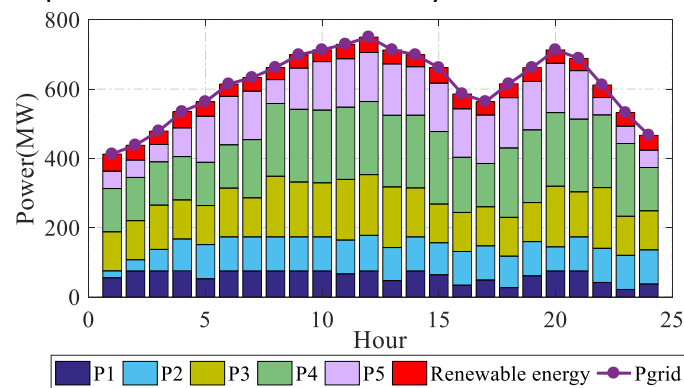


**Figure11.** Stacked bar chart of units' output and power balance constraints of Model 1 for System 1

In System 1, it is verified that the IMA algorithm combined with the wind-photovoltaic stable output strategy has better optimization effect on 5 units. For small wind and solar Systems, it can better maintain the stability of wind and solar power output power under the premise of optimizing economy and emission, which is better for small wind-solar System to maintain a stable renewable energy output while optimizing operating cost and pollutant emission.

## 5.2. System 2

System 2 contains 10 thermal power units, 3 wind turbines, 2 photovoltaic devices and 1 energy storage device, with the forecast power of wind turbines and photovoltaic devices remaining the same as in System 1. The load requirements are shown in Figure 5.

### 5.2.1. Discussion on IMA optimization algorithm in System 2

The operating cost and pollutant emission are of the same order of magnitude in System 1, so that the value of the proportional coefficient  $Q$  in fitness function (6) does not work that it is taken as 1. In System 2, the operating cost and pollutant emission are of different orders of magnitude so that proportional coefficient  $Q$  takes the value of 10. As with System 1, the value of the weight coefficient  $\omega$  is varied and the IMA algorithm is run for 200 iterations per time to obtain the set of Pareto solutions and calculate the corresponding compromise solution. This is also compared with the fitness function commonly used in the current research without the inclusion of the proportional coefficient  $Q$  to obtain another set of Pareto solution. Two sets of Pareto solutions are shown in Figure 12. The result that the Pareto solution set obtained by adding the proportional coefficient  $Q$  works better than the Pareto solution set without adding  $Q$ . For general fitness function, the fitness value of the function is still determined by the operating costs and is basically unaffected by the pollutant emission when the operating cost is much larger than the pollutant emission even if the weight coefficient  $\omega$  is added. And it is only by imputing the cost and emission to an order of magnitude that the points indicating the operating cost and pollutant emission are more linear and the resulting target value is smaller. Then the weight coefficient  $\omega$  corresponding to the compromise solution with the highest satisfaction is obtained through membership function and takes the value of 0.75.

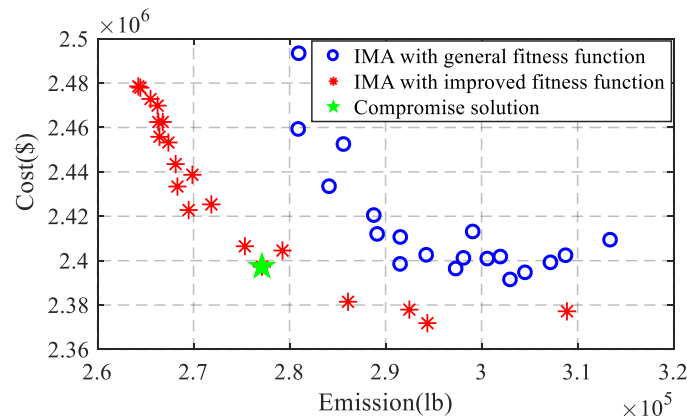


**Figure 12.** Pareto solution set for System 2

Table 7 shows the comparison of the results of IMA, MA, MFO and PSO algorithm in System 2. The MA algorithm is closer in cost and 1.99% lower in emission compared to MFO algorithm, and much better than the PSO algorithm. The results demonstrate the optimization effect of MA algorithm. Compared with MA algorithm, the cost of the IMA algorithm is reduced by 60895\$, accounting for 2.49%; and the pollutant emission is reduced by 1392lb, accounting for 0.51%. Compared with MFO algorithm and PSO algorithm, the cost of IMA algorithm is reduced by 2.38% and 4.10% respectively, and the pollutant emission is reduced by 2.48% and 13.59% respectively. As with System 1, the transmission loss of the IMA algorithm is minimum in System 2, and effectively verifying with both Systems that the optimal unit operation reduces System transmission loss.

Figure 13 shows a comparison of the operating cost and pollutant emission of four algorithms in System 2 within 24 hours. The differences are not obvious in many moments in the graph due to the large order of magnitude of costs and emissions in System 2, so some moments are selected to mark the actual data. It can still be seen that the IMA algorithm for solving HDEED problem achieves a lower value in operating cost and pollutant emission per hour, which is better than MA, MFO and PSO algorithms. At the 5th hour, the actual cost

obtained by IMA algorithm is 1404\$, 2512\$ and 3792\$ lower than that of MA, MFO and PSO algorithms respectively, even if the curves of the costs are close. The IMA algorithm is more effective in optimizing the cost when the load power drops from peak to valley compared to other algorithms. Therefore, the IMA algorithm also has advantages in System 2 for 10 thermal power units.

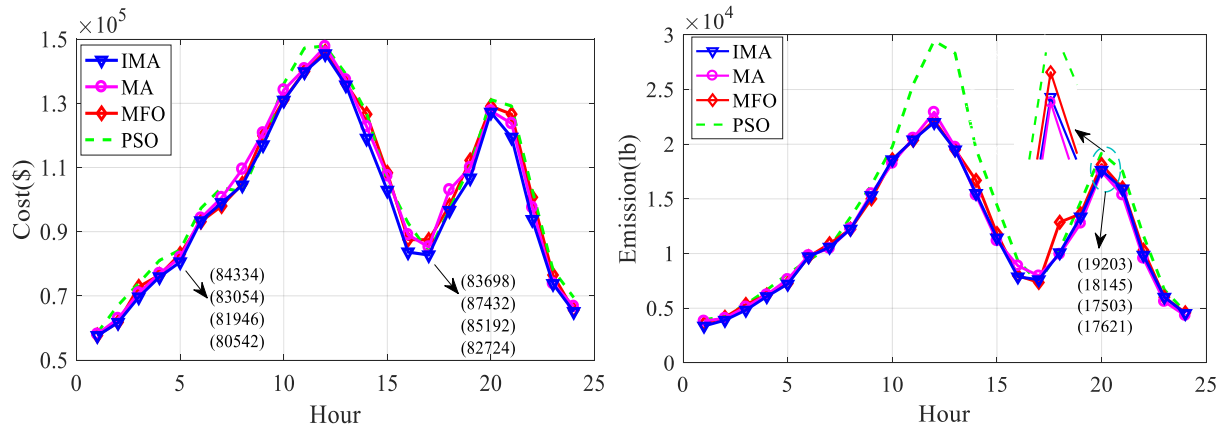


**Figure 13.** Objective curves of different algorithms for System 2

**Table 7.** Operating results of different Algorithms for System 2

Algorithms	Cost ( $10^6$ ) (\$)	Emission ( $10^5$ ) (lb)	Loss (MW)
IMA	2.3815	2.7349	1409.8485
MA	2.4424	2.7488	1439.0598
MFO	2.4396	2.8045	1452.0845
PSO	2.4832	3.1651	1521.2283

### 5.2.2. Discussion on wind and photovoltaic stability output strategy in System 2

The IMA algorithm is also applied to optimize HDEED model with wind-photovoltaic stable output strategy in System 2, and Model 1, Model 2 and Model 3 are used for comparative analysis to verify the effectiveness of wind and photovoltaic output strategy.

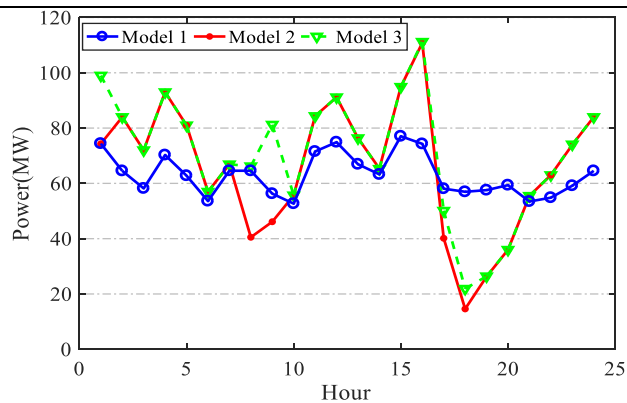
Table 8 represents the comparison of parameters of three models in System 2, including operating cost, pollutant emission, charge and discharge power and final electricity of energy storage device. The operating cost and pollutant emission of Model 1 are  $2.3941 \times 10^6$ \$ and  $2.7594 \times 10^5$ lb respectively. Model 2, which is used as a comparison, also had no significant advantage in terms of operating cost and pollutant emission. In Model 3, the discharge power is 66.5822MW and the charge power is close to 0, which indicates that the energy storage device does not play an effective regulatory role. Therefore, if only the operation cost and pollutant emission are considered, Model 1 without the wind-photovoltaic stable output strategy works better. However, in the actual situation, it is necessary to reduce the cost and pollutant emission as much as possible under the premise of assurance the stable operation of system, that makes it more important to stabilize the dispatch power of the wind and photovoltaic.

Figure 8 shows the total dispatched power of wind, photovoltaic and energy storage device of the three models in System 2. Compared with the renewable energy output data of the three models in System 1, the total output of renewable energy obtained by Model 2 and Model 3 in System 2 is the same in most of the time except for a few moments, which is more

evidence of the stability of the optimization effect of the IMA algorithm. The total dispatch power curve of Model 1 with wind-photovoltaic output strategy is more stable than that of Model 2 and Model 3. Only Model 1 is able to maintain the stability of the total output of wind, photovoltaic and energy storage device when the renewable energy power rises and falls rapidly during the period of 15.00–21.00, which is conducive to the secure and stable operation of the power grid.

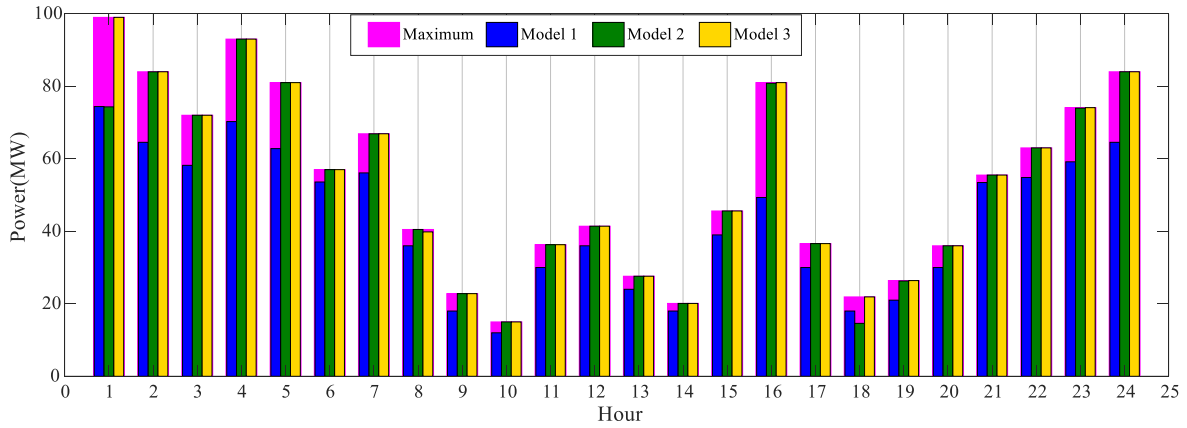
**Table 8.** Comparison of the results of three models in System 2

Model	Cost( $10^6$ )( $\$$ )	Emission( $10^5$ )(lb)	Discharge power(MW)	Charge power(MW)	Electricity(MW·h)
Model 1	2.3941	2.7594	205.4170	239.2658	81.07
Model 2	2.3884	2.7624	0	0	0
Model 3	2.3815	2.7349	66.5822	0.0911	0

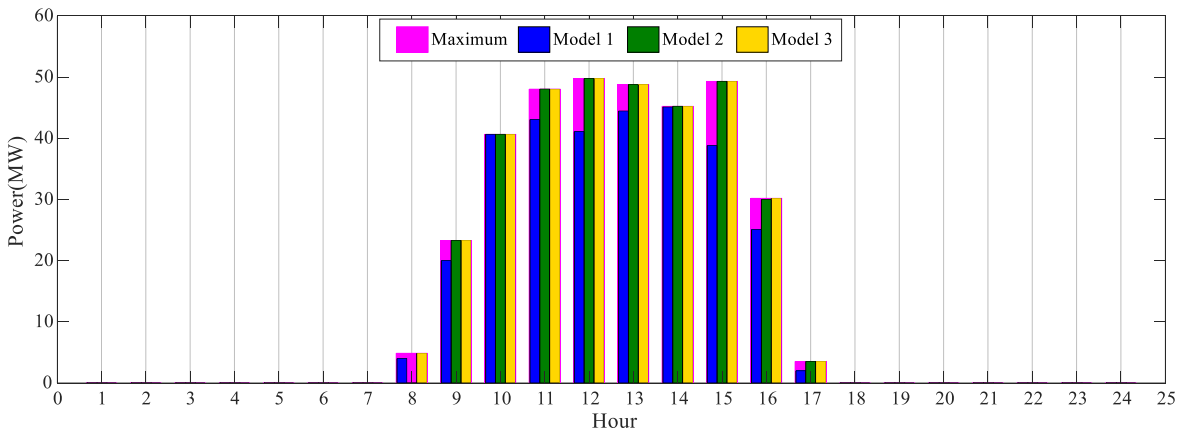


**Figure 14.** Renewable energy output of the three models in System 2

Figure 15 shows the comparison of wind power and photovoltaic power dispatched by three models of System 2 over a 24-hour period. The dispatched photovoltaic power in Model 1 has not been greatly reduced due to the stability of photovoltaic power generation. For the wind power, Model 1 reduces part of the wind power connected to the grid during the period of 0.00-5.00 and 21.00-24.00 when wind power is high. At 16<sup>th</sup> hour when the wind power fluctuates greatly, Model 1 will also reduce the dispatched power in order to stabilize the output. Compared with the predicted wind power, the dispatched power is reduced by 36.68MW, accounting for 39.11%, and the dispatched power is reduced little compared to the forecast power when wind output is low. The dispatched power of wind and photovoltaic in Model 2 and Model 3 are similar at most times. As in the case of System 1, the wind and photovoltaic power is fully integrated into the grid for consumption to reduce operating cost and pollutant emission even if the energy storage device is added to Model 3, and the energy storage device does not play a role in regulating the wind and photovoltaic power.



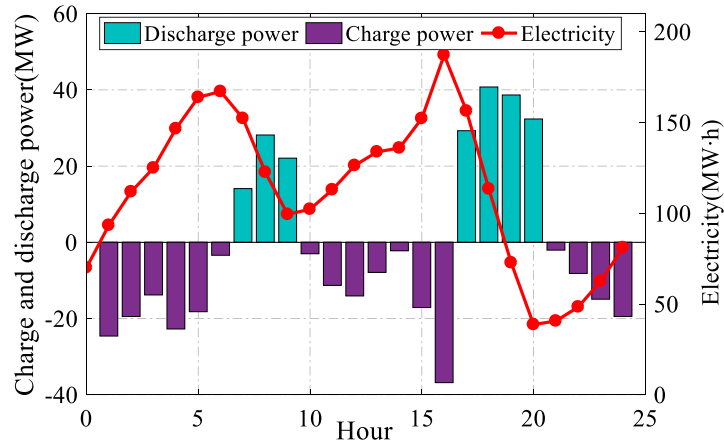
(a) Comparison of wind power



(b) Comparison of photovoltaic power

**Figure 15.** Different types of renewable energy output of the three models in System 2

Table 9 shows the optimal dispatch power for units of Model 1 in System 2. Where P1-P10 represent the power of thermal power units; PW1-PW3 represent the power of three wind turbines, and the power dispatched by wind turbines are the same under the same strategy; PV1-PV2 represent the power of photovoltaic devices, P<sub>bat</sub> represents the dispatched power of the energy storage device, and E represents the electricity of energy storage device in each hour. Figure 16 shows the optimal hourly electricity and charge and discharge power of the energy storage device corresponding to model 1 in System 2. During the morning and evening peaks, the discharge power of energy storage device will increase with the load demand. The initial electricity of energy storage device is 70MW•h for System2. The electricity of Model 1 is 81.07MW•h at the 24<sup>th</sup> hour, and the electricity of Model 3 is close to 0 according to Table 8. By comparison, only the Model 1 combined with the wind and photovoltaic output strategy is relatively close in electricity at the beginning and end moments of the dispatch, which can better meet the sustainability for energy storage device dispatch.



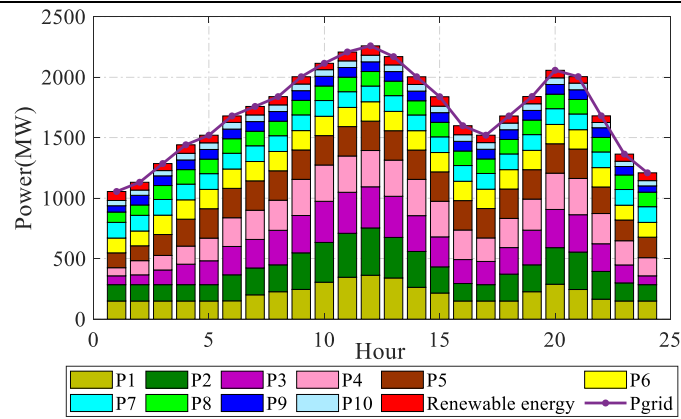
**Figure 16.** Electricity and charge and discharge power of energy storage power station in System 2

Figure 17 shows the stacked bar chart of thermal power units and renewable energy dispatched power of Model 1 in System 2. The uppermost curve represents the power grid, which is the total power of load and loss. The remaining parts represent the dispatch power of each thermal power units respectively. The change of optimal power of thermal power units is more directly by stacked bar chart under the condition of keeping the total dispatch power of wind, photovoltaic and energy storage device stable. According to the coincidence of grid power line and the top of the histogram, it shows that the power required by the grid is consistent with the power of all generation devices and also verifies that proposed model in System 2 is able to satisfy the power balance constraints.

**Table 9.** The dispatch output of each power generation device of Model 1 in System 2

Hour	P1	P2	P3	P4	P5	P6	P7	P8	P9	P10	PW1/2/PV1/ E 3 2	P_bat		
1	150.0	135.0	73.00	67.15	122.8	122.4	129.6	85.31	52.0	43.4	24.80	0.00	93.37	-
2	150.0	135.0	81.23	117.1	122.9	122.4	129.5	85.31	80.0	43.4	21.51	0.00	111.8	-
3	150.0	135.0	121.4	120.4	172.7	160.0	129.6	115.3	80.0	43.4	19.40	0.00	124.9	-
4	150.0	135.0	169.3	149.4	222.6	160.0	129.5	120.0	80.0	55.0	23.42	0.00	146.5	-
5	150.0	135.0	197.3	187.3	243.0	160.0	130.0	120.0	80.0	55.0	20.93	0.00	163.8	-
6	151.4	215.0	234.4	237.3	243.0	160.0	130.0	120.0	80.0	55.0	17.86	0.00	167.1	-3.41
7	200.9	222.1	235.8	241.2	243.0	160.0	130.0	120.0	80.0	55.0	18.70	0.00	152.2	14.09
8	226.6	222.2	285.5	248.7	243.0	160.0	130.0	120.0	80.0	55.0	12.00	0.00	122.6	28.16
9	245.7	302.2	308.7	298.7	243.0	160.0	130.0	120.0	80.0	55.0	6.00	10.0	99.39	22.09
10	305.3	328.8	340.0	300.0	243.0	160.0	130.0	120.0	80.0	55.0	4.00	20.3	102.2	-3.00
11	346.4	363.2	339.0	300.0	243.0	158.6	129.8	120.0	80.0	55.0	10.00	20.7	112.9	-
12	362.8	391.1	340.0	300.0	242.9	159.9	130.0	120.0	80.0	54.9	12.00	19.4	126.3	-
13	340.4	335.1	340.0	298.9	243.0	160.0	129.9	120.0	79.1	55.0	8.00	21.4	133.8	-7.89
14	263.1	296.2	296.0	300.0	242.5	160.0	130.0	117.2	80.0	55.0	6.00	22.6	135.9	-2.23
15	215.9	216.2	247.9	294.3	242.9	160.0	129.6	119.8	80.0	53.7	13.00	19.0	152.2	-
16	150.0	144.5	197.9	244.3	243.0	160.0	130.0	120.0	80.0	54.7	16.44	12.4	187.1	-
17	150.0	135.0	191.9	194.3	243.0	160.0	130.0	120.0	80.0	55.0	10.00	1.00	156.3	29.29
18	150.0	222.2	219.2	241.2	243.0	160.0	130.0	120.0	80.0	55.0	6.00	0.00	113.4	40.76

19	226.6	222.2	286.8	256.7	243.0	160.0	130.0	120.0	80.0	55.0	7.00	0.00	72.76	38.66
20	288.6	302.2	315.8	300.0	243.0	160.0	130.0	120.0	80.0	55.0	10.00	0.00	38.69	32.36
21	244.9	309.5	308.5	300.0	243.0	160.0	130.0	120.0	80.0	55.0	17.81	0.00	40.64	-2.06
22	164.9	229.5	228.5	250.0	219.5	160.0	129.5	120.0	80.0	43.4	18.28	0.00	48.40	-8.16
23	150.0	149.5	148.5	200.0	171.4	122.4	129.6	120.0	70.1	43.4	19.72	0.00	62.58	-
24	150.0	135.0	73.00	150.0	169.4	122.4	129.5	120.0	52.0	43.4	21.51	0.00	81.07	-



**Figure 17.** Units' output and power balance constrain of model 1 in System 2

The result is verified that the economic environmental dispatch model combined with wind-photovoltaic stable output strategy has better flexibility and controllability through two test Systems, while the combination of energy storage devices can compensate for the anti-peak characteristics of wind power to a certain extent and reduce the output of thermal power units, which can be used effectively to solve HDEED problems.

## 6. Concluding Remarks

The combination of renewable energy with thermal power units to supply power to the grid has become a development trend due to its environmental friendliness and less affected by the global energy crisis. This study analyzes the optimal configuration of power systems considering wind, photovoltaic and energy storage devices, and proposes an optimization method composed of wind- photovoltaic stable output strategy and improved MA algorithm to solve the problems of economy, environment and renewable energy output stability. The practicality of the proposed method is finally verified by using a system of 5 thermal units and 10 thermal units, and the power distribution of wind, photovoltaic and energy storage under the condition of stable output of renewable energy is analyzed in detail. The comprehensive analysis leads to the following findings.

- The MA algorithm with adaptive factor, mutation and chaos initialization method has better global search performance, and the excellent optimization ability of the IMA algorithm is verified by using unimodal function, multimodal function and composite test function.
- According to the different orders of magnitude between operating cost and pollutant emission, the proportional coefficient  $Q$  is added to the fitness function to obtain a better Pareto solution set. The test System 2 is that the improved fitness function is helpful to obtain a set of solutions with more linearity and higher correlation.
- For the test System 1 optimized by using IMA algorithm, the cost and pollutant emission are  $4.7020 \times 10^4 \$$  and  $1.7522 \times 10^4 \text{lb}$  respectively, which are 4.12%, 13.21% and 15.14% lower in terms of cost and 1.68%, 6.18% and 6.12% lower in terms of emission than the

model using MA, MFO and PSO algorithms.

- The HDEED model combined with the wind and photovoltaic output strategy is verified by using two test Systems, which makes full use of the peak-cutting and valley-filling function of the energy storage device.

The innovative contributions are described as follows: An improved IMA algorithm with excellent performance is proposed to optimize economic, environmental and stability problems; An improved fitness function is introduced to find compromise solution more accurately; The uncertainty of renewable energy output is studied and a wind-photovoltaic stability output strategy is proposed aiming at improving stability. The influence of different predicted and actual values of renewable energy output on the grid can be effectively avoided by appropriately reducing the power of renewable energy connected to the grid, so as to obtain stable output of renewable energy, which is important for the actual stable operation of electricity system.

This study contributes to improve the ability to receive clean energy while ensuring economy and stability of power grid. However, there are also some limitations, which will be addressed in future research: The prediction of renewable energy is no longer used to replace the actual value for dispatch, but to explore the impact of prediction deviation on grid power under different strategies proposed in this study; then time-of-use electricity price should be considered in dispatch model to explore the benefits of differential electricity price when energy storage is used to adjust renewable energy output.

### **Acknowledgements**

This study was supported by the key project of Tianjin Natural Science Foundation [Project No. 19JCZDJC32100] and the Natural Science Foundation of Hebei Province of China [Project No. E2018202282].

### **References**

1. Alshammari, M.E., Ramli, M.A.M. and Mehedi, I.M., 2020. An Elitist Multi-Objective Particle Swarm Optimization Algorithm for Sustainable Dynamic Economic Emission Dispatch Integrating Wind Farms. 12(18): 7253.
2. Arasomwan, M.A. and Adewumi, A.O., 2013. On the performance of linear decreasing inertia weight particle swarm optimization for global optimization. Scientific World Journal, 2013: 860289.
3. Basu, M., 2011. Economic environmental dispatch using multi-objective differential evolution. Applied Soft Computing, 11(2): 2845-2853.
4. Chen, S.Q., Kharrazi, A., Liang, S., Fath, B.D., Lenzen, M. and Yan, J.Y., 2020. Advanced approaches and applications of energy footprints toward the promotion of global sustainability. Applied Energy, 261: 9.
5. Chen, Y.X., Yu, T., Yang, B., Zhang, X.S. and Qu, K.P., 2019. Many-Objective Optimal Power Dispatch Strategy Incorporating Temporal and Spatial Distribution Control of Multiple Air Pollutants. IEEE Transactions on Industrial Informatics, 15(9): 5309-5319.
6. Chinnadurraj, C.L. and Victoire, T.A.A., 2020. Dynamic Economic Emission Dispatch Considering Wind Uncertainty Using Non-Dominated Sorting Crisscross Optimization. IEEE Access, 8: 94678-94696.
7. de Siqueira, L.M.S. and Peng, W., 2021. Control strategy to smooth wind power output

- using battery energy storage system: A review. *Journal of Energy Storage*, 35: 102252.
8. Dhiman, G., Guo, S. and Kaur, S., 2018. ED-SHO: A framework for solving nonlinear economic load power dispatch problem using spotted hyena optimizer. *Modern Physics Letters A*, 33(40).
  9. Dong, R.Y. and Wang, S.S., 2020. New Optimization Algorithm Inspired by Kernel Tricks for the Economic Emission Dispatch Problem With Valve Point. *IEEE Access*, 8: 16584-16594.
  10. Espinosa, S., Arias, D. and Yanez, M., 2017. Economic Dispatch Hydrothermal System with CO2 Emissions Constraints. *IEEE Latin America Transactions*, 15(11): 2090-2096.
  11. Evangeline, S.I. and Rathika, P., 2021. A real-time multi-objective optimization framework for wind farm integrated power systems. *Journal of Power Sources*, 498.
  12. Ganjefar, S. and Tofighi, M., 2011. Dynamic economic dispatch solution using an improved genetic algorithm with non-stationary penalty functions. *European Transactions on Electrical Power*, 21(3): 1480-1492.
  13. Gaspar, I., Castro, R. and Sousa, T., 2021. Optimisation and economic feasibility of Battery Energy Storage Systems in electricity markets: The Iberian market case study. *Journal of Cleaner Production*, 324: 129255.
  14. Hazra, S. and Roy, P.K., 2020. Optimal dispatch using moth-flame optimization for hydro-thermal-wind scheduling problem. *International Transactions on Electrical Energy Systems*, 30(8).
  15. Heffron, R.J., Korner, M.F., Schopf, M., Wagner, J. and Weibelzahl, M., 2021. The role of flexibility in the light of the COVID-19 pandemic and beyond: Contributing to a sustainable and resilient energy future in Europe. *Renewable & Sustainable Energy Reviews*, 140.
  16. Hlalele, T.G., Naidoo, R.M., Bansal, R.C. and Zhang, J., 2020. Multi-objective stochastic economic dispatch with maximal renewable penetration under renewable obligation. *Applied Energy*, 270: 115120.
  17. Huang, C., Yue, D., Xie, J., Li, Y. and Wang, K., 2016. Economic dispatch of power systems with virtual power plant based interval optimization method. *CSEE Journal of Power and Energy Systems*, 2(1): 74-80.
  18. IEA, 2021. Net Zero by 2050. International Energy Agency, Paris.
  19. Jian, L., Qian, Z., Zhao, L.G. and You, M.K., 2020. Distributed economic dispatch method for power system based on consensus. *IET Renewable Power Generation*, 14(9): 1424-1432.
  20. Jin, J.L., Zhou, P., Zhang, M.M., Yu, X.Y. and Din, H., 2018. Balancing low-carbon power dispatching strategy for wind power integrated system. *Energy*, 149: 914-924.
  21. Li, C., Zhou, H., Li, J. and Dong, Z., 2020. Economic dispatching strategy of distributed energy storage for deferring substation expansion in the distribution network with distributed generation and electric vehicle. *Journal of Cleaner Production*, 253: 119862.
  22. Li, L.L., Liu, Z.F., Tseng, M.L., Zheng, S.J. and Lim, M.K., 2021a. Improved tunicate swarm algorithm: Solving the dynamic economic emission dispatch problems. *Applied Soft Computing*, 108.
  23. Li, L.L., Shen, Q., Tseng, M.L. and Luo, S.F., 2021b. Power system hybrid dynamic economic emission dispatch with wind energy based on improved sailfish algorithm. *Journal of*

- Cleaner Production, 316.
24. Liang, H.J., Liu, Y.G., Li, F.Z. and Shen, Y.J., 2019. Dynamic Economic/Emission Dispatch Including PEVs for Peak Shaving and Valley Filling. *IEEE Transactions on Industrial Electronics*, 66(4): 2880-2890.
  25. Liu, Z.-F., Li, L.-L., Liu, Y.-W., Liu, J.-Q., Li, H.-Y. and Shen, Q., 2021. Dynamic economic emission dispatch considering renewable energy generation: A novel multi-objective optimization approach. *Energy*, 235: 121407.
  26. Ma, S.J., Wang, Y.H. and Lv, Y.H., 2018. Multiobjective Environment/Economic Power Dispatch Using Evolutionary Multiobjective Optimization. *IEEE Access*, 6: 13066-13074.
  27. Mahdi, F.P., Vasant, P., Abdullah-Al-Wadud, M., Kallimani, V. and Watada, J., 2019. Quantum-behaved bat algorithm for many-objective combined economic emission dispatch problem using cubic criterion function. *Neural Computing & Applications*, 31(10): 5857-5869.
  28. Mazzoni, S., Ooi, S., Nastasi, B. and Romagnoli, A., 2019. Energy storage technologies as techno-economic parameters for master-planning and optimal dispatch in smart multi energy systems. *Applied Energy*, 254: 113682.
  29. Mirjalili, S., 2015. Moth-flame optimization algorithm: A novel nature-inspired heuristic paradigm. *Knowledge-Based Systems*, 89: 228-249.
  30. Mohammadian, M., Lorestani, A. and Ardehali, M.M., 2018. Optimization of single and multi-areas economic dispatch problems based on evolutionary particle swarm optimization algorithm. *Energy*, 161: 710-724.
  31. Mohy-ud-din, G., 2017. Hybrid dynamic economic emission dispatch of thermal, wind, and photovoltaic power using the hybrid backtracking search algorithm with sequential quadratic programming. *Journal of Renewable and Sustainable Energy*, 9(1), 015502.
  32. Murphy, C.A., Schleifer, A. and Eurek, K., 2021. A taxonomy of systems that combine utility-scale renewable energy and energy storage technologies. *Renewable and Sustainable Energy Reviews*, 139: 110711.
  33. Nazari-Heris, M., Mohammadi-Ivatloo, B. and Gharehpetian, G.B., 2018. A comprehensive review of heuristic optimization algorithms for optimal combined heat and power dispatch from economic and environmental perspectives. *Renewable and Sustainable Energy Reviews*, 81: 2128-2143.
  34. Nemati, M., Braun, M. and Tenbohlen, S., 2018. Optimization of unit commitment and economic dispatch in microgrids based on genetic algorithm and mixed integer linear programming. *Applied Energy*, 210: 944-963.
  35. Qian, S., Wu, H. and Xu, G., 2020. An improved particle swarm optimization with clone selection principle for dynamic economic emission dispatch. *Soft Computing*, 24(20): 15249-15271.
  36. Reddy, S.S. and Bijwe, P.R., 2015. Real time economic dispatch considering renewable energy resources. *Renewable Energy*, 83: 1215-1226.
  37. Saenz, J.P., Celik, N., Xi, H., Son, Y.J. and Asfour, S., 2013. Two-stage economic and environmental load dispatching framework using particle filtering. *International Journal of Electrical Power & Energy Systems*, 48: 93-110.

38. Shi, Y. and Eberhart, R., 1998. A modified particle swarm optimizer, 1998 IEEE International Conference on Evolutionary Computation Proceedings. IEEE World Congress on Computational Intelligence (Cat. No.98TH8360), pp. 69-73.
39. Sun, W., Zhang, H., Tseng, M.L., Zhang W. and Li X., 2021. Hierarchical energy optimization management of active distribution network with multi-microgrid system, *Journal of Industrial and Production Engineering*, DOI: 10.1080/21681015.2021.1972478
40. Song, X., Wang, Y., Zhang, Z., Shen, C. and Pena-Mora, F., 2021. Economic-environmental equilibrium-based bi-level dispatch strategy towards integrated electricity and natural gas systems. *Applied Energy*, 281.
41. Soroudi, A., Rabiee, A. and Keane, A., 2017. Stochastic Real-Time Scheduling of Wind-Thermal Generation Units in an Electric Utility. *IEEE Systems Journal*, 11(3): 1622-1631.
42. Sundaram, A., 2020. Multiobjective multi-verse optimization algorithm to solve combined economic, heat and power emission dispatch problems. *Applied Soft Computing*, 91.
43. Tan, Q., Mei, S., Dai, M., Zhou, L., Wei, Y. and Ju, L., 2020. A multi-objective optimization dispatching and adaptability analysis model for wind-PV-thermal-coordinated operations considering comprehensive forecasting error distribution. *Journal of Cleaner Production*, 256: 120407.
44. Tseng, M.L., Tran, T.P.T., Ha, H.M., Bui, T.D. and Lim, M.K. (2021) Sustainable industrial and operation engineering trends and challenges Toward Industry 4.0: a data driven analysis, *Journal of Industrial and Production Engineering*, 38(8), 581-598
45. Wang, J.Y., He, X., Huang, J.J. and Chen, G., 2021. Recurrent Neural Network for Nonconvex Economic Emission Dispatch. *Journal of Modern Power Systems and Clean Energy*, 9(1): 46-55.
46. WMO, 2020. WMO Provisional Report on the State of the Global Climate 2020. World Meteorological Organization.
47. Wu, X.M., Cao, W.H., Wang, D.H. and Ding, M., 2019. A Multi-Objective Optimization Dispatch Method for Microgrid Energy Management Considering the Power Loss of Converters. *Energies*, 12(11), 2160.
48. Xie, M., Luo, W.H., Cheng, P.J., Ke, S.J., Ji, X. and Liu, M.B., 2018. Multidisciplinary collaborative optimisation-based scenarios decoupling dynamic economic dispatch with wind power. *IET Renewable Power Generation*, 12(6): 727-734.
49. Yang, L., He, D. and Li, B., 2020. A Selection Hyper-Heuristic Algorithm for Multiobjective Dynamic Economic and Environmental Load Dispatch. *Complexity*, 2020: 4939268.
50. Ye, Z., Li, X., Jiang, F., Chen, L., Wang, Y. and Dai, S., 2021. Hierarchical Optimization Economic Dispatching of Combined Wind-PV-thermal-energy Storage System Considering the Optimal Energy Abandonment Rate. *Dianwang Jishu/Power System Technology*, 45(6): 2270-2279.
51. Zervoudakis, K. and Tsafarakis, S., 2020. A mayfly optimization algorithm. *Computers & Industrial Engineering*, 145.

## Appendix

**Table A1.** Generation device coefficients in System 1

Unit	$p$	$a$	$q$	$\varphi$	$h$	$\theta$	$b$	$c$	$o$	$g$	$p^U$	$p^D$	$p^{\max}$	$p^{\min}$
1	-0.805	0.0080	0.018	0.02846	0.042	0.6550	2.0	25	80	100	30	30	75	10
2	-0.555	0.0030	0.015	0.02446	0.040	0.5773	1.8	60	50	140	30	30	125	20
3	-1.355	0.0012	0.0105	0.02270	0.038	0.4968	2.1	100	60	160	40	40	175	30
4	-0.600	0.0010	0.008	0.01948	0.037	0.4860	2.0	120	45	180	50	50	250	40
5	-0.555	0.0015	0.012	0.02075	0.035	0.5035	1.8	40	30	200	50	50	300	50

**Table A2.** Generation device coefficients in System 2

Unit	$p$	$\varphi$	$q$	$h$	$a$	$\theta$	$b$	$o$	$g$	$c$	$p^U$	$p^D$	$p^{\max}$	$p^{\min}$
1	-2.4444	0.0207	0.0312	0.041	0.1524	0.5035	38.5397	103.3908	450	786.7988	80	80	470	150
2	-2.4444	0.0207	0.012	0.036	0.1058	0.5035	46.1591	103.3908	600	451.3251	80	80	470	135
3	-4.0695	0.0202	0.0509	0.028	0.0280	0.4968	40.3965	300.3910	320	1049.9977	80	80	340	73
4	-4.0695	0.0202	0.0509	0.052	0.0354	0.4968	38.3055	300.3910	260	1243.5311	50	50	300	60
5	-3.8132	0.0200	0.0344	0.063	0.0211	0.4972	36.3278	320.0006	280	1658.5696	50	50	243	73
6	-3.8132	0.0200	0.0344	0.048	0.0179	0.4972	38.3055	320.0006	310	1356.6592	50	50	160	57
7	-3.9023	0.0214	0.0465	0.086	0.0121	0.5163	36.5104	330.0056	300	1450.7045	30	30	130	20
8	-3.9023	0.0214	0.0465	0.082	0.0121	0.5163	36.5104	330.0056	240	1450.7045	30	30	120	47
9	-3.9524	0.0234	0.0465	0.098	0.1090	0.5475	39.5804	350.0056	270	1455.6056	30	30	80	20
10	-3.9864	0.0234	0.0470	0.094	0.1295	0.5475	40.5407	360.0012	380	1469.4026	30	30	55	10